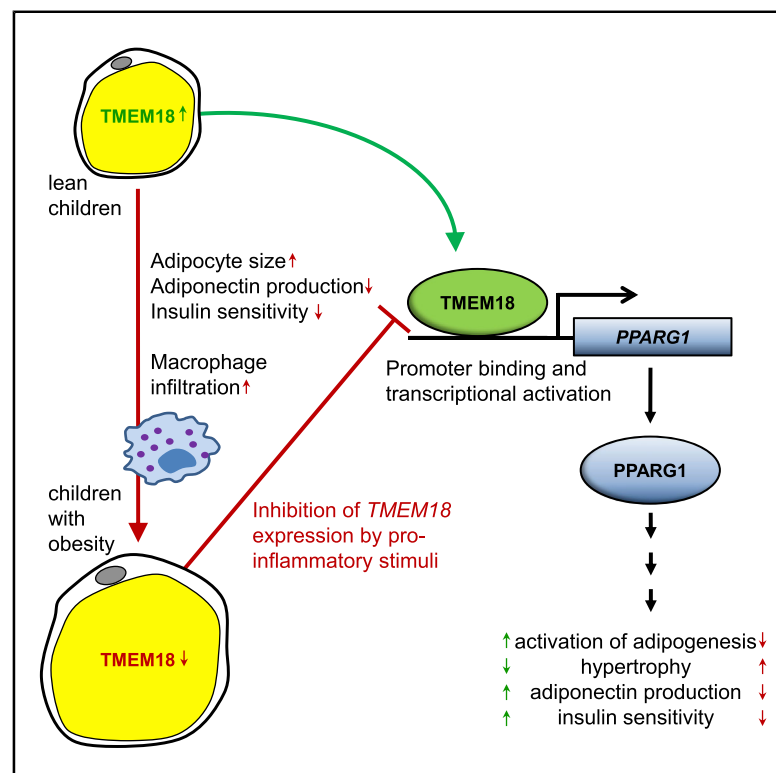


The Obesity-Susceptibility Gene *TMEM18* Promotes Adipogenesis through Activation of *PPARG*

Graphical Abstract



Authors

Kathrin Landgraf, Nora Klötting, Martin Gericke, ..., Matthias Blüher, Wieland Kiess, Antje Körner

Correspondence

kathrin.landgraf@medizin.uni-leipzig.de (K.L.),
antje.koerner@medizin.uni-leipzig.de (A.K.)

In Brief

Landgraf et al. show that the obesity-susceptibility gene *TMEM18* is of critical functional importance for adipose tissue biology. *TMEM18* promotes adipogenesis by activating *PPARG1* and thereby metabolically beneficial hyperplasia. The link between *TMEM18* and *PPARG1* is dysregulated in obesity and related inflammatory and metabolic parameters in children.

Highlights

- *TMEM18* expression is essential for adipocyte formation *in vitro* and *in vivo*
- *TMEM18* activates *PPARG* by upregulating *PPARG1* promoter activity
- *TMEM18* and *PPARG1* are dysregulated with obesity and adipose tissue dysfunction



Report

The Obesity-Susceptibility Gene *TMEM18* Promotes Adipogenesis through Activation of *PPARG*

Kathrin Landgraf,^{1,*} Nora Klötting,^{2,3} Martin Gericke,⁴ Nitzan Maixner,⁵ Esther Guiu-Jurado,³ Markus Scholz,^{6,7} A. Veronica Witte,⁸ Frauke Beyer,⁸ Julian T. Schwartz,¹ Martin Lacher,⁹ Arno Villringer,⁸ Peter Kovacs,³ Assaf Rudich,⁵ Matthias Blüher,^{2,3} Wieland Kiess,¹ and Antje Körner^{1,10,*}

¹Center for Pediatric Research Leipzig (CPL), Hospital for Children & Adolescents, University of Leipzig, Leipzig 04103, Germany

²Helmholtz Institute for Metabolic, Obesity and Vascular Research (HI-MAG) of the Helmholtz Zentrum München at the University of Leipzig and University Hospital Leipzig, Leipzig 04103, Germany

³Medical Department III-Endocrinology, Nephrology, Rheumatology, University of Leipzig, Leipzig 04103, Germany

⁴Institute of Anatomy, University of Leipzig, Leipzig 04103, Germany

⁵Department of Clinical Biochemistry and Pharmacology, Ben-Gurion University of the Negev, Beer-Sheva 8410501, Israel

⁶Institute for Medical Informatics, Statistics and Epidemiology, University of Leipzig, Leipzig 04103, Germany

⁷LIFE Research Center for Civilization Diseases, University of Leipzig, Leipzig 04103, Germany

⁸Department of Neurology, Max Planck Institute for Human Cognitive and Brain Sciences, Leipzig 04103, Germany

⁹Department of Pediatric Surgery, University of Leipzig, Leipzig 04103, Germany

¹⁰Lead Contact

*Correspondence: kathrin.landgraf@medizin.uni-leipzig.de (K.L.), antje.koerner@medizin.uni-leipzig.de (A.K.)

<https://doi.org/10.1016/j.celrep.2020.108295>

SUMMARY

TMEM18 is the strongest candidate for childhood obesity identified from GWASs, yet as for most GWAS-derived obesity-susceptibility genes, the functional mechanism remains elusive. We here investigate the relevance of *TMEM18* for adipose tissue development and obesity. We demonstrate that adipocyte *TMEM18* expression is downregulated in children with obesity. Functionally, downregulation of *TMEM18* impairs adipocyte formation in zebrafish and in human preadipocytes, indicating that *TMEM18* is important for adipocyte differentiation *in vivo* and *in vitro*. On the molecular level, *TMEM18* activates *PPARG*, particularly upregulating *PPARG1* promoter activity, and this activation is repressed by inflammatory stimuli. The relationship between *TMEM18* and *PPARG1* is also evident in adipocytes of children and is clinically associated with obesity and adipocyte hypertrophy, inflammation, and insulin resistance. Our findings indicate a role of *TMEM18* as an upstream regulator of *PPARG* signaling driving healthy adipogenesis, which is dysregulated with adipose tissue dysfunction and obesity.

INTRODUCTION

Obesity manifests early in life (Geserick et al., 2018) and is characterized by excessive accumulation of adipose tissue (AT) because of increased adipocyte size and/or number, with new adipocytes arising from proliferation and differentiation of adipose progenitor cells (Landgraf et al., 2015). Genome-wide association studies (GWASs) suggested transmembrane protein 18 (*TMEM18*) as a strong candidate for development and progression of obesity (Fall and Ingelsson, 2014).

As for most identified obesity-susceptibility genes, action related to central nervous system for *TMEM18* was initially postulated based on prior observations that *TMEM18* was involved in neural stem cell migration (Juvansuu et al., 2008). However, it remains inconclusive as to whether and in what direction central *TMEM18* expression is related to food intake or body weight in rodents (Gutierrez-Aguilar et al., 2012; Larder et al., 2017).

A potential functional relevance of *TMEM18* in AT has so far been widely neglected, despite indications that *Tmem18* expression is decreased in AT of mice (Yoganathan et al., 2012) and adult patients with obesity (Rohde et al., 2014). Based on these observations, we

hypothesized that *TMEM18* may have a direct role in AT accumulation and that alterations in *TMEM18* expression may affect adipocyte formation and expression of adipogenic marker genes. Of particular interest is *PPARG*, a transcription factor, which is the master regulator of adipogenesis, driving expression of critical genes necessary for adipocyte differentiation and function, such as *LPL*, *FABP4*, and *LIPE* (Rosen et al., 1999; Siersbaek et al., 2010).

Therefore, the aim of the present study was to decipher the functional relevance of *TMEM18* for AT accumulation in development and in the context of obesity. Particularly, we investigated the importance of *TMEM18* for adipocyte formation from adipose progenitor cells and analyzed the regulatory mechanisms underlying *TMEM18* function.

RESULTS

Adipocyte *TMEM18* Expression Is Decreased with Obesity and AT Dysfunction in Children

We first investigated whether obesity-risk variants are linked to *TMEM18* expression in AT of children (Table S1). We selected three independent variants, rs7561317, rs17729501, and



rs10168696, located in different regions within or close to the *TMEM18* locus, which had been associated with obesity in large cross-sectional GWASs (Thorleifsson et al., 2009; Wiemerslage et al., 2016; Willer et al., 2009). We detected an association of rs7561317 and rs17729501, but not rs10168696, with adipocyte *TMEM18* expression in lean children (Table S2; Figure 1A). We further evaluated the association of the variant rs7561317 with eating behavior. For this, we used the population-based Leipzig Research Center for Civilization Diseases (LIFE) Child and LIFE Adult studies, which are human epidemiological datasets with both genotyping and different measures of eating behavior available. We confirmed an average higher body mass index (BMI) of 0.57 kg/m² in risk versus non-risk allele-carrying adults ($t_{1140} = 2.01$, 95% confidence interval [CI] of the difference [0.035, 1.1], $p = 0.037$) and a higher BMI standard deviation score (SDS) of 0.15 in risk-carrying children ($t_{924} = 1.97$, 95% CI of the difference [0.3, 0.0006], $p = 0.047$). Yet we did not find effects on traits related to eating behavior: In children, restraint, eating, weight, and shape concern were not different between genotype groups (all $Z < 1.22$, $p > 0.22$). Similarly, food avoidance emotional disorder (FAED), selective eating, and functional dysphagia were comparable (all $Z < 0.46$, $p > 0.65$). In adults, hunger, disinhibition or cognitive restraint measures as analyzed by multivariate comparison corrected for age and sex ($N = 1,144$, multivariate ANOVA, Pillai's trace test statistics, $F_{3,1138} = 1.3$, $p = 0.28$), and Yale Food Addiction Scale symptom score distributions did not differ among genotypes (Mann-Whitney U test: $Z = -0.009$, $p = 0.99$). Hence, *TMEM18* is expressed in AT, and expression may be altered according to risk genotype, whereas we did not find the risk genotype to be related to central traits regulating appetite.

Independent of genotype, *TMEM18* expression was lower in adipocytes compared with stroma-vascular fraction (SVF) cells (Figure 1A). Adipocyte *TMEM18* mRNA levels did not correlate with age ($R = -0.229$, $p = 0.168$), puberty ($R = -0.150$, $p = 0.406$), or gender ($7,970 \pm 679$ in females versus $8,877 \pm 750$ in males, $p = 0.380$) in lean children, indicating that there is no association with physical development that might bias analyses. However, *TMEM18* expression was reduced in adipocytes of children with obesity compared with lean children (Figure 1B) to a similar extent as shown for AT of adults (Bernhard et al., 2013). In addition to the association with BMI SDS (Figure 1C), *TMEM18* expression decreased with emerging signs of obesity-related AT dysfunction and with clinical obesity sequelae, such as insulin resistance (Figures 1D–1G).

***TMEM18* Is Conserved in Zebrafish and Is Coexpressed with *pparg* in AT**

Based on our previous observation of *TMEM18* deficiency impairing adipocyte differentiation *in vitro* (Bernhard et al., 2013), we hypothesized that *TMEM18* has a role in adipogenesis, which we studied in zebrafish *in vivo*. *TMEM18* is conserved in zebrafish (Figure S1A) and ubiquitously expressed throughout different tissues, including visceral adipose and brain tissues (Figure S1B), resembling expression in humans (Bernhard et al., 2013) and mice (Figure S2A). During development, *tmem18* expression increased from 4 h to 9 days post-fertilization (dpf) (Figure S1C). Investigating spatial expression,

tmem18 mRNA was initially localized to pharyngeal arches, head, and swimbladder, whereas at 9 dpf, *tmem18* expression was restricted to the abdominal swimbladder region, in which *pparg* is expressed and the first AT develops (Figure S1D).

***Tmem18* Knockdown Inhibits *pparg* Expression and Adipocyte Development in Zebrafish**

To address whether *tmem18* is a regulator of adipocyte development in zebrafish, we used a morpholino-mediated knockdown approach (Figures 2A and 2B). *Tmem18* knockdown led to a reduction in adipocyte number (Figures 2C and 2D) and to a reduced percentage of zebrafish larvae containing adipocytes (Figure 2D), which was not caused by systemic effects on development per se (Figure 2E) or by detrimental effects on liver and intestinal development (Figure 2F). Reduction of adipocyte number was unlikely to be secondary to reduced food intake, because we did not observe alterations in eating behavior (Figure 2G). However, we did observe decreased *pparg* expression in *tmem18* morphants, and inhibition of adipocyte formation and *pparg* expression were restored by coinjection of *tmem18* mRNA (Figure 2H), whereas there was no effect on other early regulators of adipocyte differentiation (Figure 2I). Analyses of late adipocyte markers revealed that only *lpl-b* expression showed a trend toward downregulation after *tmem18* knockdown at 5 and 9 dpf as time points relevant for adipocyte formation, which was not statistically significant (Figure 2J).

***TMEM18* Upregulates Transcription from the *PPARG1* Promoter**

Concomitant expression and colocalization results suggest that *TMEM18* might be involved in *PPARG* activation. Supporting this hypothesis are observations that *TMEM18* protein is present in both cytoplasm and nucleus and acts as a transcription factor (Jurvansuu and Goldman, 2011), whereas a recent study reported that *TMEM18* does not localize to the nucleus to act as a transcription factor (Larder et al., 2017). We detected endogenous *TMEM18* protein in both cytoplasm and nucleus of human adipose progenitor cells before and after adipocyte differentiation (Figures S2B and S2C).

We went on testing whether *TMEM18* is involved in *PPARG* activation. *TMEM18* overexpression in undifferentiated 3T3-L1 cells caused a doubling of *PPARG1*, but not *PPARG2*, promoter activity (Figure 3A). By generating deletion constructs of the *PPARG1* promoter (Figure 3B), we demonstrated that the distal region (−1,765 to −1,464) is essential for *TMEM18*-mediated *PPARG1* activation (Figure 3C). We confirmed the presence of *TMEM18* in a complex with the 3' region of the distal *PPARG1* promoter using chromatin immunoprecipitation in undifferentiated Simpson-Golabi-Behmel syndrome (SGBS) cells overexpressing *TMEM18* (Figure 3D).

To verify the relevance of the interaction between *TMEM18* and *PPARG*, we analyzed the effect of *TMEM18* knockdown on lipid accumulation and *PPARG1/2* expression during differentiation of murine 3T3-L1 and human SGBS cells *in vitro*. *TMEM18* knockdown led to a reduction of adipocyte differentiation (Figure 3E; Figure S2D), which was accompanied by reduced *PPARG1* expression before adipogenic induction and subsequently during later stages of adipocyte differentiation (Figure 3F;

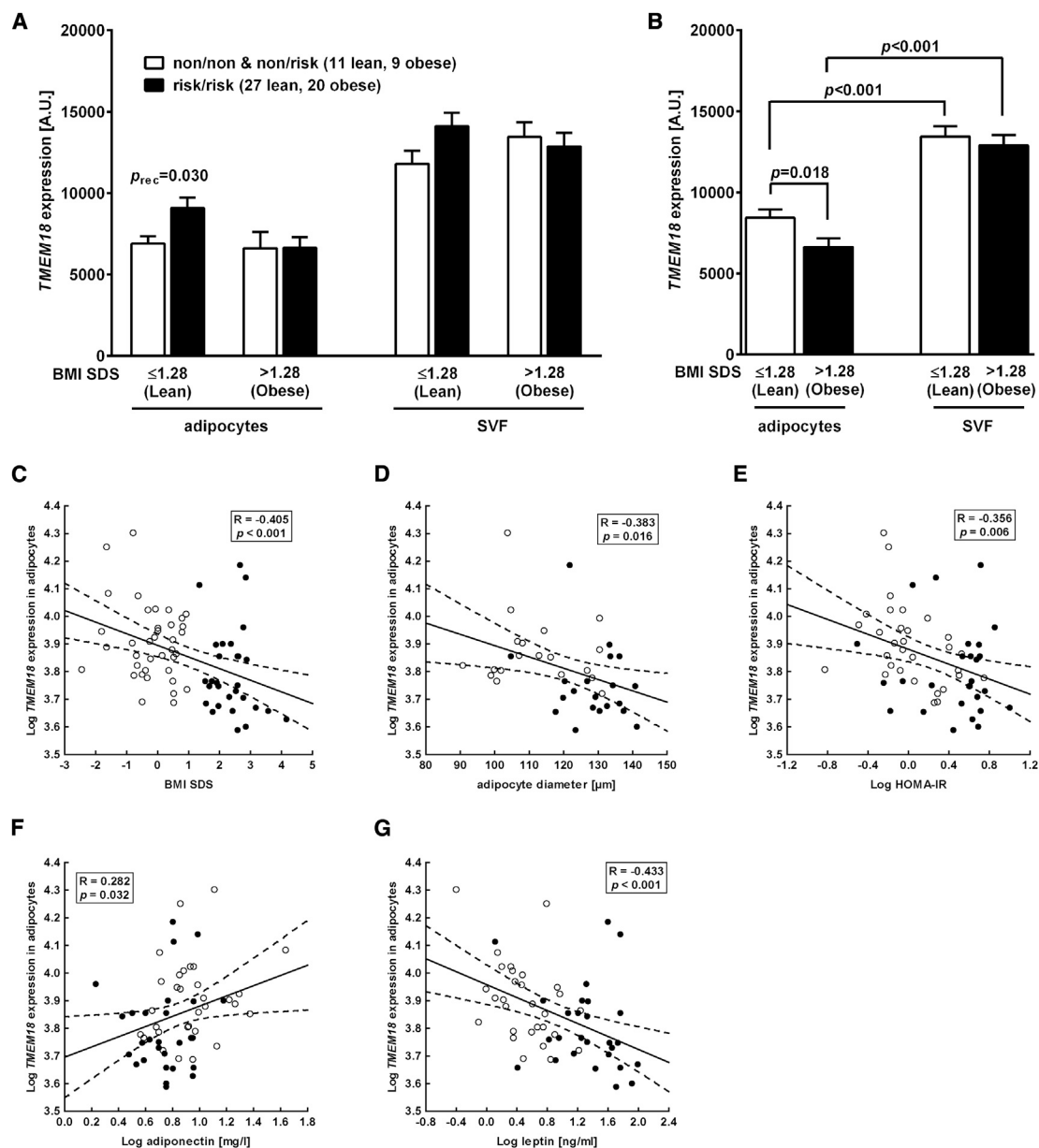


Figure 1. Expression of *TMEM18* in AT of Children and Association with *TMEM18* Risk Variants and Obesity

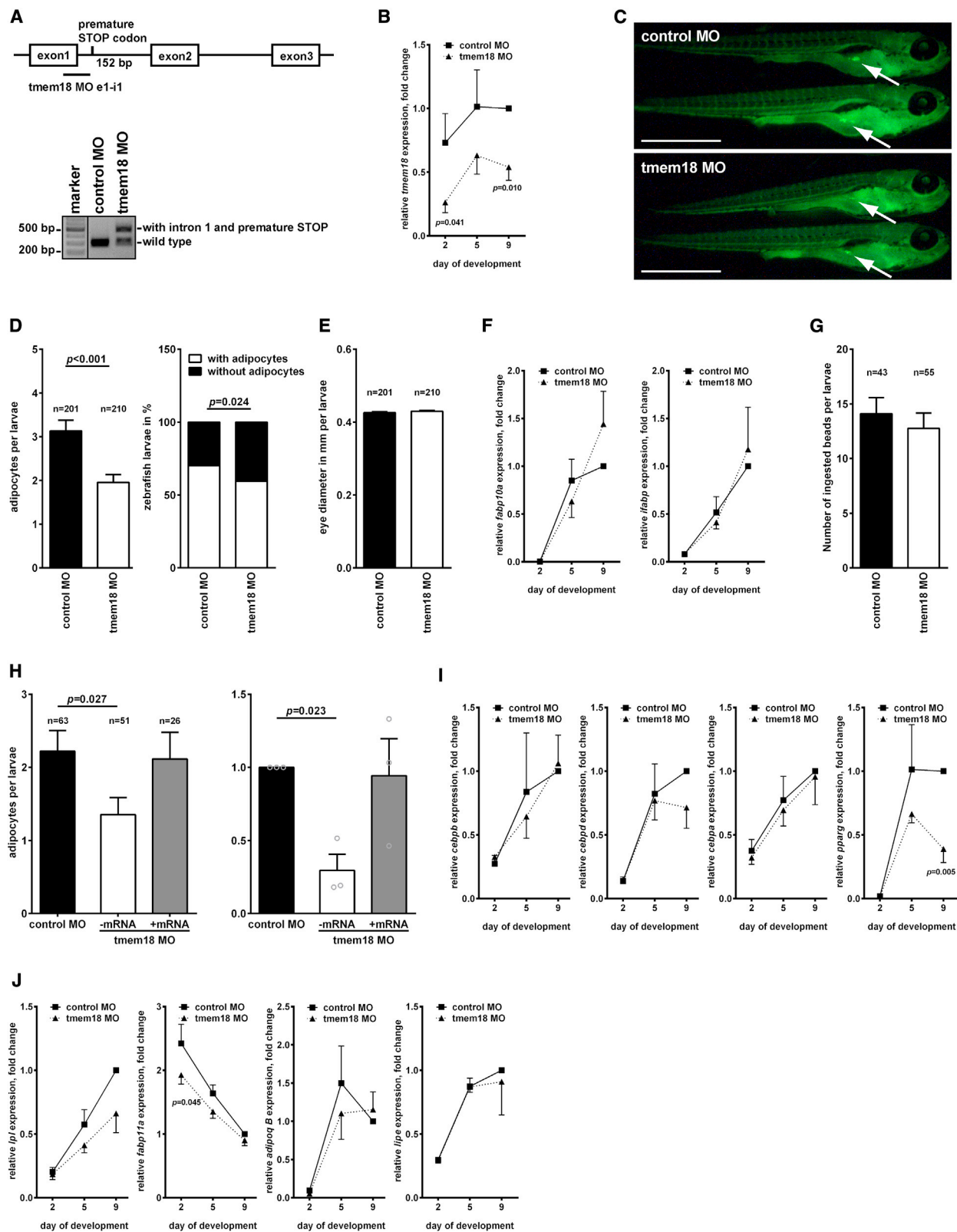
(A) Adipocyte *TMEM18* expression was increased in lean children homozygous for the *TMEM18* rs7561317 risk allele. A recessive model for inheritance of the risk allele was assumed, and homozygous and heterozygous non-risk allele carriers were combined. Data are presented as mean \pm SEM. Significant p values ($p < 0.05$) are given.

(B–G) *TMEM18* expression was lower in adipocytes compared with stroma-vascular fraction (SVF) cells (paired t test, significant p values are given). Adipocyte expression, but not SVF *TMEM18* expression, was reduced in children with obesity and associated with BMI SDS (C), adipocyte diameter (D), HOMA-IR (E), and adiponectin (F) and leptin (G) serum levels.

For analyses, children who were overweight (BMI SDS > 1.28) and children with obesity (BMI SDS > 1.88) were combined in one group designated as obese. Lean children are represented as open circles; children with obesity are represented as closed circles. See also Tables S1 and S2.

Figure S2E). In contrast, *PPARG2* expression and expression of the early adipogenic marker genes (and *PPARG* activators) *CEBPB*, *CEBPD*, *CEBPA*, and *SREBF1* were not affected by *TMEM18* knockdown in human SGBS cells except at late stages of adipocyte differentiation. Furthermore, *PPARG* target genes, i.e., *LPL*, *FABP4*, *PLIN*, *ADIPOQ*, *LIPE*, and *SLC2A4*, showed

downregulation at late stages of adipocyte differentiation after *TMEM18* inhibition, which was mirroring the effect of *PPARG* downregulation (Figure 3F). On the protein level, *TMEM18* knockdown resulted in *PPARG1* downregulation. *PPARG2* protein expression was restricted to day 8 of adipocyte differentiation and was reduced by *TMEM18* inhibition (Figure 3G). Finally,



(legend on next page)

our findings of a positive correlation between *TMEM18* and *PPARG1* expression, but not *PPARG2* expression, in adipocytes from children indicate that the interplay between *TMEM18* and *PPARG1* is of physiological relevance in human AT (Figure 3H).

PPARG1 Expression Correlates with TMEM18 Expression and Clinical Phenotypes in Humans

Beyond the association with *TMEM18* expression, adipocyte *PPARG1* expression correlated with the extent of obesity (Figure S3A) and early markers of metabolic impairment (Figure S3B–S3D), phenocopying the association of *TMEM18* with these parameters and suggesting that *TMEM18*-mediated specific regulation of *PPARG1* might be effective in AT of children *in vivo*.

Looking at the association of *TMEM18* expression differentially for *PPARG1* and *PPARG2* in AT samples from 529 adults, we observed a similar association of *TMEM18* expression primarily with *PPARG1* (subcutaneous: $R = 0.579$, $p < 0.001$; visceral: $R = 0.614$, $p < 0.001$), and with *PPARG2* (subcutaneous: $R = 0.417$, $p < 0.001$; visceral: $R = 0.524$, $p < 0.001$).

TMEM18 Is a Mediator of Inflammation-Induced PPARG1 Repression in Adipocytes

The downregulation of *PPARG* expression and activity related to obesity-associated adipocyte hypertrophy is supposed to be driven by an inflammatory milieu (Guilherme et al., 2008). Therefore, we evaluated the association of adipocyte *TMEM18*, *PPARG1*, and *PPARG2* expression with AT inflammation in subcutaneous AT of children. Adipocyte *TMEM18* expression decreased with increasing macrophage number, along with increasing *CD68* mRNA expression, and was lower in AT with macrophages forming crown-like structures (CLSs) (Figure S4A). In particular, we found the reduction of *TMEM18* expression in AT with CLSs similar to that for *PPARG1*, whereas the association with SVF *CD68* expression or macrophage number was not as clear for *PPARG1* (Figure S4B) or *PPARG2* (Figure S4C).

Based on the concordant regulation of *TMEM18* and *PPARG1* in association with surrogate markers of AT inflammation, we investigated whether *TMEM18* expression was regulated by pro-inflammatory stimuli *in vitro*. Treatment of human SGBS cells at day 10 of differentiation with macrophage-conditioned medium led to a reduction in *TMEM18*, *PPARG1*, and *PPARG2*

expression (Figure 4A). IL-4 (interleukin-4)-mediated induction of M2 polarization of macrophages in AT explants from mice did not affect *Tmem18* or *Pparg* expression, whereas induction of the M1 macrophage phenotype by tumor necrosis factor alpha (TNF- α) decreased *Tmem18* and *Pparg1* expression, but not *Pparg2* expression (Figure 4B). We next tested whether this effect might be partially caused by a direct effect of TNF- α on adipocytes. Treatment of human adipocytes with the TNF-superfamily cytokines TRAIL (TNF-related apoptosis-inducing ligand), TL1A (TNF-like ligand 1A), and TNF- α caused a reduction in *TMEM18*, *PPARG1*, and *PPARG2* expression (Figures 4C and 4D). Importantly, TNF- α -mediated reduction in *PPARG1* expression levels in differentiated SGBS cells could be partially rescued by *TMEM18* overexpression, which was not the case for *PPARG2* (Figure 4E).

DISCUSSION

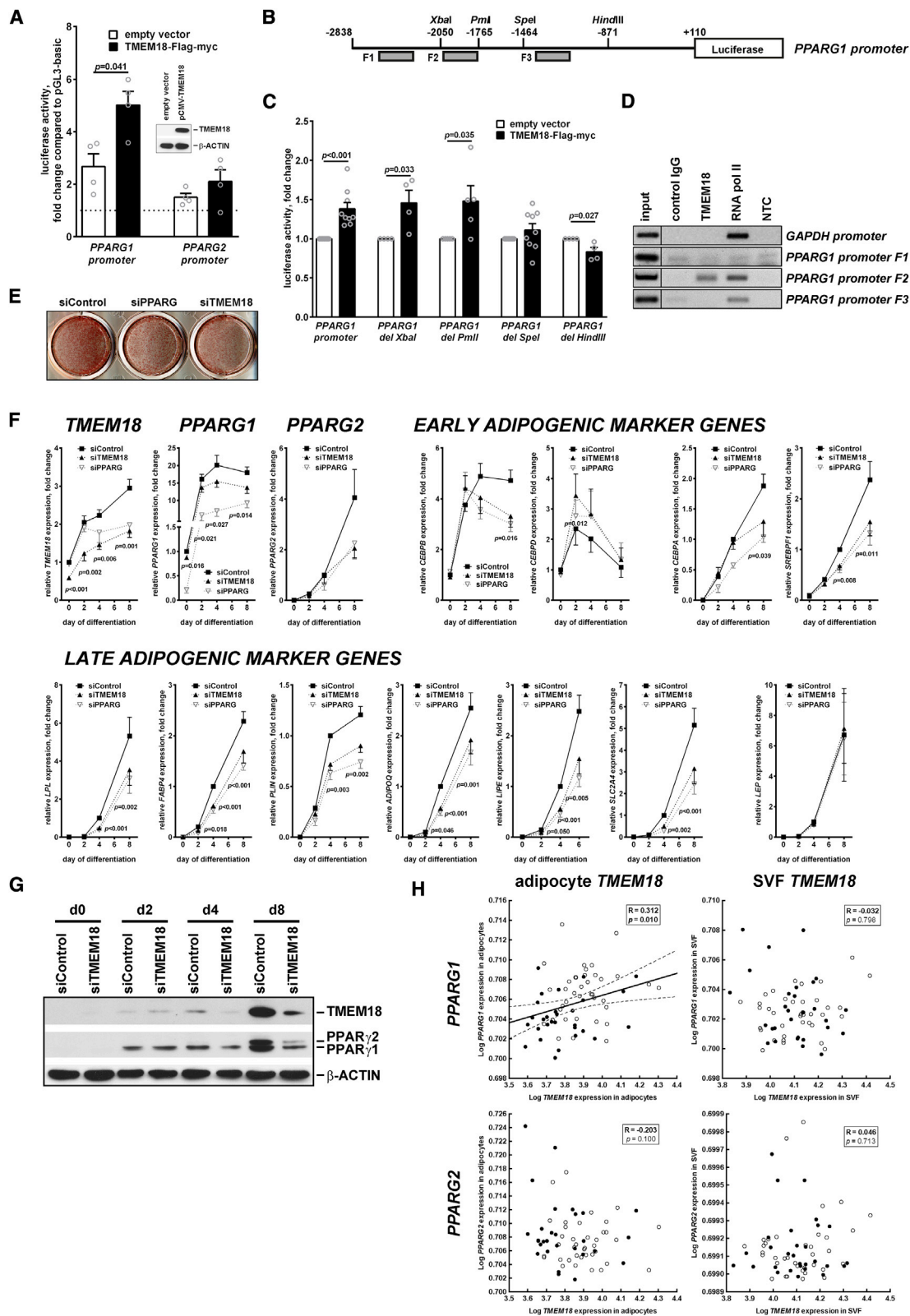
TMEM18 is the strongest candidate for childhood obesity identified from GWASs, but as for most GWAS-derived obesity-susceptibility genes, the functional mechanism remains elusive. In rodents, a putative link between hypothalamic *TMEM18* expression with food intake or body weight has been claimed (Gutierrez-Aguilar et al., 2012; Yoganathan et al., 2012), yet the direction of effects remains controversial (Larder et al., 2017). Our results do not support the hypothesis that *TMEM18* strongly affects eating behavior. We did not see an association of *TMEM18* obesity risk variants with the behavioral traits of hunger, disinhibition, or food addiction in children or adults. Coherently, in zebrafish, *tmem18* deficiency did not affect food intake. Even though we cannot entirely exclude an effect of *TMEM18* on dietary intake in humans based on our data, previous results from a Greek childhood cohort indicate that the *TMEM18* obesity risk genotype is not associated with energy intake (Rask-Andersen et al., 2012). Hence, overall there is no conclusive evidence that *TMEM18* might be a central regulator of food intake and obesity.

Earlier studies have addressed whether obesity risk variants in *TMEM18* are linked to its expression in whole AT samples, but they did not find an association (Bernhard et al., 2013; Lu et al., 2016; Rohde et al., 2014). Here, we provide evidence that obesity-associated *TMEM18* variants correlate with

Figure 2. Tmem18 Is Essential for Adipocyte Formation in Zebrafish Larvae

- Expression of *tmem18* was targeted by injection of splice donor site morpholino (MO).
- Injection of *tmem18* MO resulted in a reduction of *tmem18* expression to about 30% in 2-day-old zebrafish and was maintained until 9 dpf.
- At 9 dpf, larvae were stained with Nile red. Representative images are shown (scale bar, 1 mm). White arrows point to visceral adipocytes. Adipocytes of larvae stained with Nile red at 9 dpf were counted, and eye diameter was determined (combined results of 3 independent experiments).
- Tmem18* knockdown led to a reduction in the number of visceral adipocytes and the percentage of zebrafish larvae containing adipocytes (stacked bar plot, chi-square test).
- There was no difference in eye diameter between *tmem18*-morphant and control zebrafish at 9 dpf.
- Tmem18* knockdown did not affect expression of marker genes for liver (*fabp10a*) and intestinal development (*ifabp*).
- Tmem18*-morphant zebrafish larvae did not show alterations in eating behavior at 9 dpf (combined results of 3 independent experiments).
- Tmem18* knockdown was associated with reduced *pparg* expression at 9 dpf, and the effect on adipocyte formation and *pparg* expression were rescued by coinjection of *tmem18* mRNA.
- Expression of early adipogenic regulators was determined during zebrafish development. Only *pparg* expression was reduced in 9 dpf zebrafish larvae after *tmem18* MO injection.
- Tmem18* knockdown did not result in alterations of late adipocyte marker gene expression at 5 and 9 dpf.

Data are mean \pm SEM. Significant p values ($p < 0.05$) are given. hpf/dpf, hours/days post-fertilization. See also Figure S1.



(legend on next page)

adipocyte *TMEM18* expression in lean children, indicating that these variants might affect mechanisms acting within AT. Beyond genetic association, lower *TMEM18* expression in adipocytes was observed in children with obesity and associated with AT dysfunction and clinical obesity sequelae. A similar regulatory pattern has been described for other well-characterized regulators of adipocyte development, e.g., *PPARG* (Guilherme et al., 2008), nourishing the hypothesis that *TMEM18* might play a role in adipogenesis.

To prove this *in vivo*, we employed the zebrafish, which has emerged as a suitable model for the analyses of processes related to AT accumulation (Schlegel and Gut, 2015). In line with the association of *TMEM18* with AT function and dysfunction in humans, our zebrafish studies demonstrated that *tmem18* is not only colocalized with *pparg* at sites where AT emerges but also important for adipocyte formation and *pparg* expression *in vivo*. In contrast to what may have been expected from human and mouse studies showing that the *FABP4* is a *PPARG* target gene, we did not detect downregulation of the zebrafish ortholog *fabp11a*. This might be because for expression analyses, we used whole zebrafish larvae, and in contrast to mammalian *FABP4*, the zebrafish ortholog is not expressed in AT only but shows prominent expression in other tissues, e.g., eye, heart, and muscle. Hence, *TMEM18* affects adipogenesis potentially by direct or indirect functional interaction with *PPARG*.

In humans, *PPARG* exists in two protein isoforms, *PPARG1* and *PPARG2*, which are generated by alternate transcription start sites and alternative splicing (Fajas et al., 1997). Our results indicate that *TMEM18* specifically activates transcription from the *PPARG1* promoter and that this is not mediated by an indirect effect on early adipogenic marker genes known to be involved in the molecular induction of *PPARG1*. Considering that *PPARG1*, but not *PPARG2*, is expressed during early stages of adipose progenitor cell differentiation (Cristancho and Lazar, 2011), one might speculate that *TMEM18* is particularly important for the early phase of adipogenic conversion.

Reassuringly, we detected a positive correlation between *TMEM18* and *PPARG1* expression in human AT, indicating that *TMEM18*-mediated regulation of *PPARG1* is effective *in vivo*.

Importantly, *TMEM18* and *PPARG1* expression were similarly downregulated in children with obesity. A decrease in *PPARG* activity in the obese state has been associated with pathogenesis of the metabolic syndrome (Ruan et al., 2002; Zhang et al., 1996). It has been suggested that adipocyte hypertrophy induces an inflammatory milieu, which leads to *PPARG* downregulation and hence inhibition of *PPARG* target genes involved in glucose and lipid metabolism (Guilherme et al., 2008). Supporting this notion, we show that inflammatory stimuli cause a reduction of *PPARG* paralleled by a reduction of *TMEM18* expression in AT explants in mice and humans.

The *PPARG* target gene adiponectin has been implicated to be a mediator of insulin sensitivity. Adiponectin mRNA and serum levels are decreased in obesity and insulin resistance (Körner et al., 2005; Landgraf et al., 2015). In line with this, we detected a correlation of both lower *TMEM18* and *PPARG1* expression with increased adipocyte size, lower adiponectin levels, and higher homeostasis model assessment of insulin resistance (HOMA-IR) values. We provide evidence that *TMEM18* downregulation might be one mechanism involved in downregulation of adipocyte *PPARG1* expression in the state of AT inflammation. These data support our hypothesis that *TMEM18* is a regulator of *PPARG*-driven adipogenesis and a mediator of obesity-related inflammation causing AT dysfunction, altered adipokine secretion, and obesity progression *in vivo*.

A limitation of our study is that we did not identify the exact molecular mechanism of *TMEM18*-mediated *PPARG1* activation. Whether *TMEM18* is directly or indirectly involved in the activation of *PPARG1* expression remains elusive and needs to be elaborated in detail in future studies. Nevertheless, we provide comprehensive and coherent evidence for *TMEM18* promoting adipogenesis *in vitro*, *in vivo*, and *ex vivo* in humans and the association of *TMEM18* expression with *PPARG1* activation.

In conclusion, we show here that the obesity gene *TMEM18* is essential for adipocyte formation and is involved in regulation of *PPARG1* expression. The coherent downregulation of *TMEM18* and *PPARG1* in response to inflammatory stimuli indicates that *TMEM18* is a mediator of inflammation-induced dysregulation

Figure 3. *TMEM18* Activates Transcription from the *PPARG1* Promoter

- (A) Overexpression of *TMEM18* in undifferentiated 3T3-L1 cells led to enhanced *PPARG1* promoter activity in luciferase reporter assays ($n = 4$). *TMEM18* overexpression in 3T3-L1 preadipocytes was confirmed by immunoblotting (inset).
- (B) Schematic overview on restriction sites for generation of *PPARG1* promoter deletion constructs. Locations of amplicons F1, F2, and F3 for chromatin immunoprecipitation (ChIP) are indicated.
- (C) Deletion constructs were tested for luciferase activity in the presence or absence of *TMEM18* in undifferentiated 3T3-L1 cells. The distal region of the *PPARG1* promoter is essential for transcriptional activation by *TMEM18* ($n = 4$ –9 biological replicates each measured in duplicates).
- (D) *TMEM18* coprecipitated with *PPARG1* promoter F2 chromatin, but not F1 or F3 chromatin, as shown by ChIP analyses in undifferentiated SGBS preadipocytes overexpressing *TMEM18*. Precipitation of RNA polymerase II served as positive control. Representative images are shown.
- (E) SGBS adipocyte differentiation was reduced after knockdown of *PPARG* and *TMEM18* as indicated by Oil red O staining at day 8.
- (F) *TMEM18* knockdown reduced *PPARG1* expression during early and late adipocyte differentiation of SGBS cells and *PPARG2* expression during late adipocyte differentiation. Expression of early adipogenic markers *CEBPB*, *CEBPD*, *CEBPA*, and *SREBF1* was not affected by *TMEM18* knockdown except at late stages of adipocyte differentiation. The *PPARG* target genes *LPL*, *FABP4*, *PLIN*, *ADIPOQ*, *LIPE*, and *SLC2A4* showed downregulation at late stages of adipocyte differentiation after *TMEM18* inhibition, which was mirroring the effect of *PPARG* downregulation ($n = 7$).
- (G) *TMEM18* knockdown led to a reduction of *TMEM18* and *PPARG* protein levels from day 4 of adipogenesis of SGBS cells.
- (H) *PPARG1* expression, but not *PPARG2* expression, was positively correlated with *TMEM18* expression in adipocytes from lean children (open circles) and children with obesity (closed circles).

Data in barplots are mean \pm SEM. Significant p values are indicated ($p < 0.05$). See also Figures S2 and S3.

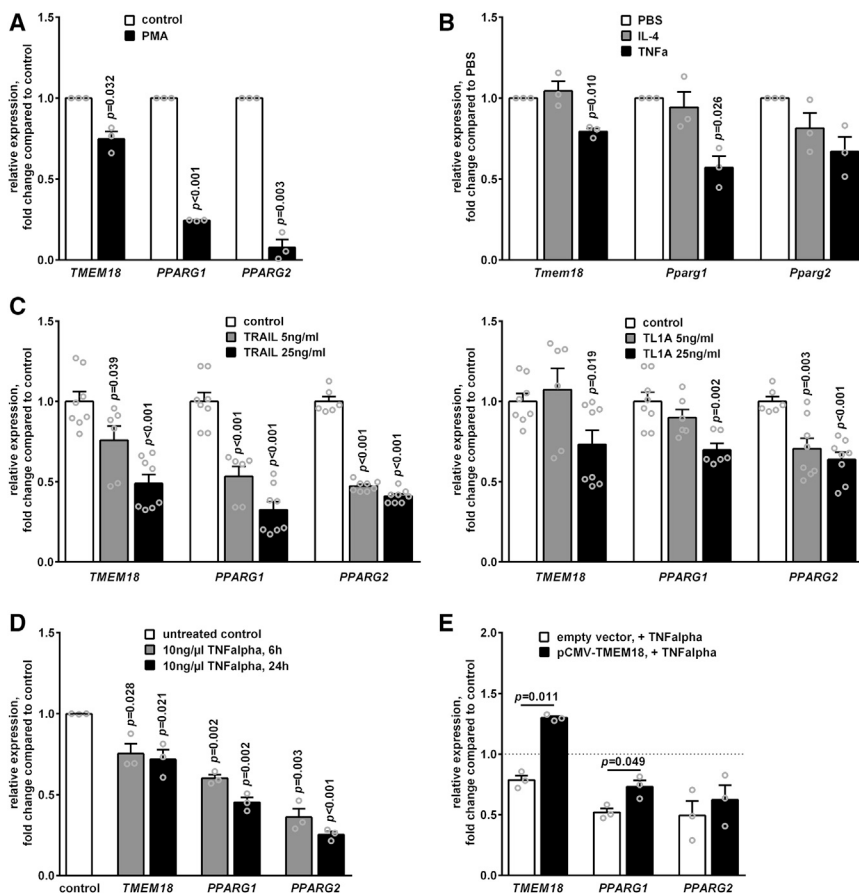


Figure 4. *TMEM18* and *PPARG1* Are Regulated by Inflammatory Stimuli in Adipocytes of Humans and Mice

(A) Treatment of human SGBS cells at day 10 of differentiation with conditioned medium from phorbol 12-myristate 13-acetate (PMA)-activated THP-1 macrophages resulted in a reduction in *TMEM18*, *PPARG1*, and *PPARG2* expression (n = 3).

(B) Although induction of M1 polarization of macrophages in AT explants from mice with IL-4 did not affect *Tmem18* or *Pparg* expression, induction of M2 polarization with TNF-α resulted in decreased *Tmem18* and *Pparg1* expression, but not *Pparg2* expression (n = 3).

(C) Treatment of differentiated human chub-s7 adipocytes with TRAIL and TL1A led to a dose-dependent reduction in *TMEM18*, *PPARG1*, and *PPARG2* expression, with *PPARG1* mirroring changes in *TMEM18* more accurately.

(D) Treatment of differentiated SGBS cells with TNF-α led to a reduction in *TMEM18*, *PPARG1*, and *PPARG2* expression (n = 3).

(E) TNF-α-mediated reduction in *PPARG1* expression in SGBS cells at day 8 of differentiation was rescued by *TMEM18* overexpression, which was not the case for *PPARG2*. Results are given as fold change compared with untreated control cells (dotted line).

Data are given as mean ± SEM. Significant p values are indicated. See also Figure S4.

of *PPARG1* associated with AT dysfunction and metabolic alterations in the obese state.

STAR★METHODS

Detailed methods are provided in the online version of this paper and include the following:

- KEY RESOURCES TABLE
- RESOURCE AVAILABILITY
 - Lead Contact
 - Materials Availability
 - Data and Code Availability
- EXPERIMENTAL MODEL AND SUBJECT DETAILS
 - Leipzig AT Childhood cohort
 - LIFE Child study cohort
 - LIFE Adult study cohort
 - Animal models and maintenance
 - Cell lines and culture conditions
- METHOD DETAILS
 - Eating behavior and *TMEM18* genotype
 - RNA isolation and RT-PCR analysis
 - *In situ* hybridization analysis
 - Morpholino injection of zebrafish embryos

- Nile red staining of zebrafish larvae
- Eating behavior of zebrafish larvae
- *In vitro* adipocyte differentiation
- Protein extraction and immunoblotting
- Immunocytochemistry
- siRNA-mediated knockdown
- Luciferase reporter assay
- Chromatin immunoprecipitation (ChIP)
- Treatment of cells with macrophage conditioned media
- IL-4 and TNFα treatment of AT explants
- TRAIL and TL1A treatment of chub-s7 adipocytes
- TNFα treatment of differentiated SGBS cells
- QUANTIFICATION AND STATISTICAL ANALYSIS

SUPPLEMENTAL INFORMATION

Supplemental Information can be found online at <https://doi.org/10.1016/j.celrep.2020.108295>.

ACKNOWLEDGMENTS

We thank Antje Berthold for technical assistance and Johan Auwerx and Yann Gibert for providing plasmids. Furthermore, we thank Steffi G. Riedel-Heller, Tobias Luck, Francisca S. Rodriguez, Matthias L. Schroeter, Anke Tönjes, and Michael Stumvoll. This work was supported by grants from the Deutsche

Forschungsgemeinschaft (DFG)–SFB 1052/2 – 2020–209933838 projects C05 (to A.K.), A01 (to A.V.), B01 (to M.B.), B02 (to A.R.), B03 (to P.K.), and B04 (to N.K.); the Federal Ministry of Education and Research (BMBF), Germany, FKZ 01EO1501 (IFB AdiposityDiseases); the University of Leipzig (formel-1-program) (to K.L.); and LIFE (Leipzig Research Center for Civilization Diseases, University of Leipzig), which is funded by means of the European Union, the European Regional Development Fund (ERDF), and the Free State of Saxony within the framework of the excellence initiative (projects 713-241202, 14505/2470, and 14575/2470).

AUTHOR CONTRIBUTIONS

Conceptualization, K.L. and A.K.; Methodology, K.L., N.K., M.G., N.M., E.G.-J., M.S., A.V.W., and F.B.; Formal Analysis, K.L., M.S., A.V.W., F.B., and P.K.; Investigation, K.L., N.K., M.G., N.M., and E.G.-J.; Resources, J.T.S., M.L., A.V., A.R., M.B., W.K., and A.K.; Writing – Original Draft, K.L. and A.K.; Writing – Review & Editing, K.L., N.K., M.G., N.M., E.G.-J., M.S., A.V.W., F.B., J.T.S., M.L., A.V., P.K., A.R., M.B., W.K., and A.K.; Supervision, K.L. and A.K.; Funding Acquisition, K.L. and A.K.

DECLARATION OF INTERESTS

The authors declare no competing interests.

Received: October 18, 2019

Revised: August 25, 2020

Accepted: September 30, 2020

Published: October 20, 2020

SUPPORTING CITATIONS

The following references appear in the Supplemental Information: Bruedigam et al. (2008); Hall et al. (2012); Lin et al. (2014).

REFERENCES

Bernhard, F., Landgraf, K., Klötting, N., Berthold, A., Büttner, P., Friebe, D., Kiess, W., Kovacs, P., Blüher, M., and Körner, A. (2013). Functional relevance of genes implicated by obesity genome-wide association study signals for human adipocyte biology. *Diabetologia* 56, 311–322.

Bond, M.J., McDowell, A.J., and Wilkinson, J.Y. (2001). The measurement of dietary restraint, disinhibition and hunger: an examination of the factor structure of the Three Factor Eating Questionnaire (TFEQ). *Int. J. Obes. Relat. Metab. Disord.* 25, 900–906.

Braune, J., Weyer, U., Hobusch, C., Mauer, J., Brüning, J.C., Bechmann, I., and Gericke, M. (2017). IL-6 Regulates M2 Polarization and Local Proliferation of Adipose Tissue Macrophages in Obesity. *J. Immunol.* 198, 2927–2934.

Bruedigam, C., Koedam, M., Chiba, H., Eijken, M., and van Leeuwen, J.P. (2008). Evidence for multiple peroxisome proliferator-activated receptor gamma transcripts in bone: fine-tuning by hormonal regulation and mRNA stability. *FEBS Lett.* 582, 1618–1624.

Cappelleri, J.C., Bushmakina, A.G., Gerber, R.A., Leidy, N.K., Sexton, C.C., Lowe, M.R., and Karlsson, J. (2009). Psychometric analysis of the Three-Factor Eating Questionnaire-R21: results from a large diverse sample of obese and non-obese participants. *Int. J. Obes.* 33, 611–620.

Cristancho, A.G., and Lazar, M.A. (2011). Forming functional fat: a growing understanding of adipocyte differentiation. *Nat. Rev. Mol. Cell Biol.* 12, 722–734.

Dietrich, A., Federbusch, M., Grellmann, C., Villringer, A., and Horstmann, A. (2014). Body weight status, eating behavior, sensitivity to reward/punishment, and gender: relationships and interdependencies. *Front. Psychol.* 5, 1073.

Fajas, L., Auboeuf, D., Raspé, E., Schoonjans, K., Lefebvre, A.M., Saladin, R., Najib, J., Laville, M., Fruchart, J.C., Deeb, S., et al. (1997). The organization, promoter analysis, and expression of the human PPARgamma gene. *J. Biol. Chem.* 272, 18779–18789.

Fall, T., and Ingelsson, E. (2014). Genome-wide association studies of obesity and metabolic syndrome. *Mol. Cell. Endocrinol.* 382, 740–757.

Farber, S.A., Pack, M., Ho, S.Y., Johnson, I.D., Wagner, D.S., Dosch, R., Mullins, M.C., Hendrickson, H.S., Hendrickson, E.K., and Halpern, M.E. (2001). Genetic analysis of digestive physiology using fluorescent phospholipid reporters. *Science* 292, 1385–1388.

Flynn, E.J., 3rd, Trent, C.M., and Rawls, J.F. (2009). Ontogeny and nutritional control of adipogenesis in zebrafish (*Danio rerio*). *J. Lipid Res.* 50, 1641–1652.

García-García, I., Horstmann, A., Jurado, M.A., Garolera, M., Chaudhry, S.J., Margulies, D.S., Villringer, A., and Neumann, J. (2014). Reward processing in obesity, substance addiction and non-substance addiction. *Obes. Rev.* 15, 853–869.

Gearhardt, A.N., Corbin, W.R., and Brownell, K.D. (2009). Preliminary validation of the Yale Food Addiction Scale. *Appetite* 52, 430–436.

Geserick, M., Vogel, M., Gausche, R., Lipek, T., Spielau, U., Keller, E., Pfäffle, R., Kiess, W., and Körner, A. (2018). Acceleration of BMI in Early Childhood and Risk of Sustained Obesity. *N. Engl. J. Med.* 379, 1303–1312.

Guilherme, A., Virbasius, J.V., Puri, V., and Czech, M.P. (2008). Adipocyte dysfunction linking obesity to insulin resistance and type 2 diabetes. *Nat. Rev. Mol. Cell Biol.* 9, 367–377.

Gutierrez-Aguilar, R., Kim, D.H., Woods, S.C., and Seeley, R.J. (2012). Expression of new loci associated with obesity in diet-induced obese rats: from genetics to physiology. *Obesity (Silver Spring)* 20, 306–312.

Hall, C.J., Flores, M.V., Oehlers, S.H., Sanderson, L.E., Lam, E.Y., Crosier, K.E., and Crosier, P.S. (2012). Infection-responsive expansion of the hematopoietic stem and progenitor cell compartment in zebrafish is dependent upon inducible nitric oxide. *Cell Stem Cell* 10, 198–209.

Hauptmann, G., and Gerster, T. (1994). Two-color whole-mount *in situ* hybridization to vertebrate and *Drosophila* embryos. *Trends Genet.* 10, 266.

Hilbert, A., Buerger, A., Hartmann, A.S., Spenner, K., Czaja, J., and Warschburger, P. (2013). Psychometric evaluation of the eating disorder examination adapted for children. *Eur. Eat. Disord. Rev.* 27, 330–339.

Jurvansuu, J.M., and Goldman, A. (2011). Obesity risk gene TMEM18 encodes a sequence-specific DNA-binding protein. *PLoS ONE* 6, e25317.

Jurvansuu, J., Zhao, Y., Leung, D.S.Y., Boulaire, J., Yu, Y.H., Ahmed, S., and Wang, S. (2008). Transmembrane protein 18 enhances the tropism of neural stem cells for glioma cells. *Cancer Res.* 68, 4614–4622.

Kimmel, C.B., Ballard, W.W., Kimmel, S.R., Ullmann, B., and Schilling, T.F. (1995). Stages of embryonic development of the zebrafish. *Dev. Dyn.* 203, 253–310.

Körner, A., Wabitsch, M., Seidel, B., Fischer-Posovszky, P., Berthold, A., Stumvoll, M., Blüher, M., Kratzsch, J., and Kiess, W. (2005). Adiponectin expression in humans is dependent on differentiation of adipocytes and down-regulated by humoral serum components of high molecular weight. *Biochem. Biophys. Res. Commun.* 337, 540–550.

Landgraf, K., Bollig, F., Trowe, M.O., Besenbeck, B., Ebert, C., Kruspe, D., Kispert, A., Hänel, F., and Englert, C. (2010). Sipl1 and Rbck1 are novel Eya1-binding proteins with a role in craniofacial development. *Mol. Cell. Biol.* 30, 5764–5775.

Landgraf, K., Friebe, D., Ullrich, T., Kratzsch, J., Ditttrich, K., Herberth, G., Adams, V., Kiess, W., Erbs, S., and Körner, A. (2012). Chemerin as a mediator between obesity and vascular inflammation in children. *J. Clin. Endocrinol. Metab.* 97, E556–E564.

Landgraf, K., Rockstroh, D., Wagner, I.V., Weise, S., Tauscher, R., Schwartz, J.T., Löffler, D., Bühligen, U., Wojan, M., Till, H., et al. (2015). Evidence of early alterations in adipose tissue biology and function and its association with obesity-related inflammation and insulin resistance in children. *Diabetes* 64, 1249–1261.

Landgraf, K., Scholz, M., Kovacs, P., Kiess, W., and Körner, A. (2016). FTO Obesity Risk Variants Are Linked to Adipocyte IRX3 Expression and BMI of Children—Relevance of FTO Variants to Defend Body Weight in Lean Children? *PLoS ONE* 11, e0161739.

- Langhardt, J., Fiehmig, G., Klötting, N., Lehmann, S., Ebert, T., Kern, M., Schön, M.R., Gärtner, D., Lohmann, T., Dressler, M., et al. (2018). Effects of Weight Loss on Glutathione Peroxidase 3 Serum Concentrations and Adipose Tissue Expression in Human Obesity. *Obes. Facts* 11, 475–490.
- Larder, R., Sim, M.F.M., Gulati, P., Antrobus, R., Tung, Y.C.L., Rimmington, D., Ayuso, E., Poxel-Wolf, J., Lam, B.Y.H., Dias, C., et al. (2017). Obesity-associated gene *TMEM18* has a role in the central control of appetite and body weight regulation. *Proc. Natl. Acad. Sci. USA* 114, 9421–9426.
- Lin, T.Y., Chou, C.F., Chung, H.Y., Chiang, C.Y., Li, C.H., Wu, J.L., Lin, H.J., Pai, T.W., Hu, C.H., and Tzou, W.S. (2014). Hypoxia-inducible factor 2 alpha is essential for hepatic outgrowth and functions via the regulation of leg1 transcription in the zebrafish embryo. *PLoS ONE* 9, e101980.
- Loeffler, M., Engel, C., Ahnert, P., Alfermann, D., Arelin, K., Baber, R., Beutner, F., Binder, H., Brähler, E., Burkhardt, R., et al. (2015). The LIFE-Adult-Study: objectives and design of a population-based cohort study with 10,000 deeply phenotyped adults in Germany. *BMC Public Health* 15, 691.
- Lu, Y., Day, F.R., Gustafsson, S., Buchkovich, M.L., Na, J., Bataille, V., Cousminer, D.L., Dastani, Z., Drong, A.W., Esko, T., et al. (2016). New loci for body fat percentage reveal link between adiposity and cardiometabolic disease risk. *Nat. Commun.* 7, 10495.
- Matthews, D.R., Hosker, J.P., Rudenski, A.S., Naylor, B.A., Treacher, D.F., and Turner, R.C. (1985). Homeostasis model assessment: insulin resistance and beta-cell function from fasting plasma glucose and insulin concentrations in man. *Diabetologia* 28, 412–419.
- Musharraf, A., Kruspe, D., Tomasch, J., Besenbeck, B., Englert, C., and Landgraf, K. (2014). BOR-syndrome-associated *Eya1* mutations lead to enhanced proteasomal degradation of *Eya1* protein. *PLoS ONE* 9, e87407.
- Neville, M.J., Collins, J.M., Gloyn, A.L., McCarthy, M.I., and Karpe, F. (2011). Comprehensive human adipose tissue mRNA and microRNA endogenous control selection for quantitative real-time-PCR normalization. *Obesity (Silver Spring)* 19, 888–892.
- Rask-Andersen, M., Jacobsson, J.A., Moschonis, G., Chavan, R.A., Sikder, M.A., Allén, E., Alsiö, J., Chrousos, G.P., Manios, Y., Fredriksson, R., and Schiöth, H.B. (2012). Association of *TMEM18* variants with BMI and waist circumference in children and correlation of mRNA expression in the PFC with body weight in rats. *Eur. J. Hum. Genet.* 20, 192–197.
- Rockstroh, D., Landgraf, K., Wagner, I.V., Gesing, J., Tauscher, R., Lakowa, N., Kiess, W., Bühligen, U., Wojan, M., Till, H., et al. (2015). Direct evidence of brown adipocytes in different fat depots in children. *PLoS ONE* 10, e0117841.
- Rohde, K., Keller, M., Klös, M., Schleinitz, D., Dietrich, A., Schön, M.R., Gärtner, D., Lohmann, T., Dreßler, M., Stumvoll, M., et al. (2014). Adipose tissue depot specific promoter methylation of *TMEM18*. *J. Mol. Med. (Berl.)* 92, 881–888.
- Rosen, E.D., Sarraf, P., Troy, A.E., Bradwin, G., Moore, K., Milstone, D.S., Spiegelman, B.M., and Mortensen, R.M. (1999). PPAR gamma is required for the differentiation of adipose tissue *in vivo* and *in vitro*. *Mol. Cell* 4, 611–617.
- Ruan, H., Hacohen, N., Golub, T.R., Van Parijs, L., and Lodish, H.F. (2002). Tumor necrosis factor-alpha suppresses adipocyte-specific genes and activates expression of preadipocyte genes in 3T3-L1 adipocytes: nuclear factor-kappaB activation by TNF-alpha is obligatory. *Diabetes* 51, 1319–1336.
- Sasmono, R.T., Oceandy, D., Pollard, J.W., Tong, W., Pavli, P., Wainwright, B.J., Ostrowski, M.C., Himes, S.R., and Hume, D.A. (2003). A macrophage colony-stimulating factor receptor-green fluorescent protein transgene is expressed throughout the mononuclear phagocyte system of the mouse. *Blood* 101, 1155–1163.
- Schlegel, A., and Gut, P. (2015). Metabolic insights from zebrafish genetics, physiology, and chemical biology. *Cell. Mol. Life Sci.* 72, 2249–2260.
- Siersbaek, R., Nielsen, R., and Mandrup, S. (2010). PPARgamma in adipocyte differentiation and metabolism—novel insights from genome-wide studies. *FEBS Lett.* 584, 3242–3249.
- Stunkard, A.J., and Messick, S. (1985). The three-factor eating questionnaire to measure dietary restraint, disinhibition and hunger. *J. Psychosom. Res.* 29, 71–83.
- Thorleifsson, G., Walters, G.B., Gudbjartsson, D.F., Steinthorsdottir, V., Sullem, P., Helgadóttir, A., Styrkarsdóttir, U., Gretarsdóttir, S., Thorlacius, S., Jonsdóttir, I., et al. (2009). Genome-wide association yields new sequence variants at seven loci that associate with measures of obesity. *Nat. Genet.* 41, 18–24.
- Wabitsch, M., Brenner, R.E., Melzner, I., Braun, M., Möller, P., Heinze, E., Debatin, K.M., and Hauner, H. (2001). Characterization of a human preadipocyte cell strain with high capacity for adipose differentiation. *Int. J. Obes. Relat. Metab. Disord.* 25, 8–15.
- Wiemerslage, L., Gohel, P.A., Maestri, G., Hilmarsson, T.G., Mickael, M., Fredriksson, R., Williams, M.J., and Schiöth, H.B. (2016). The *Drosophila* ortholog of *TMEM18* regulates insulin and glucagon-like signaling. *J. Endocrinol.* 229, 233–243.
- Willer, C.J., Speliotes, E.K., Loos, R.J., Li, S., Lindgren, C.M., Heid, I.M., Berndt, S.I., Elliott, A.L., Jackson, A.U., Lamina, C., et al.; Wellcome Trust Case Control Consortium; Genetic Investigation of ANthropometric Traits Consortium (2009). Six new loci associated with body mass index highlight a neuronal influence on body weight regulation. *Nat. Genet.* 41, 25–34.
- Yoganathan, P., Karunakaran, S., Ho, M.M., and Clee, S.M. (2012). Nutritional regulation of genome-wide association obesity genes in a tissue-dependent manner. *Nutr. Metab. (Lond.)* 9, 65.
- Zebisch, K., Voigt, V., Wabitsch, M., and Brandsch, M. (2012). Protocol for effective differentiation of 3T3-L1 cells to adipocytes. *Anal. Biochem.* 425, 88–90.
- Zhang, B., Berger, J., Hu, E., Szalkowski, D., White-Carrington, S., Spiegelman, B.M., and Moller, D.E. (1996). Negative regulation of peroxisome proliferator-activated receptor-gamma gene expression contributes to the antiadipogenic effects of tumor necrosis factor-alpha. *Mol. Endocrinol.* 10, 1457–1466.

STAR★METHODS

KEY RESOURCES TABLE

REAGENT or RESOURCE	SOURCE	IDENTIFIER
Antibodies		
Rb pAb to Tmem18	abcam	Cat# ab100954, Lot: GR108123-1
PPARgamma Rabbit mAb C26H12	Cell Signaling	Cat# 2435S, Lot: 4; RRID:AB_2166051
Rb pAb to betaActin	abcam	Cat# ab8227, Lot: GR245058-1; RRID: AB_2305186
GFP Rabbit Ab	Cell Signaling	Cat# 2555, Lot: 2; RRID: AB_10692764
c-Jun Rabbit mAb 60A8	Cell Signaling	Cat# 9165S, Lot:11; RRID: AB_2130165
Glucose-6-Phosphate Dehydrogenase A	Cell Signaling	Cat# 8866S, Lot: 1; RRID: AB_10827744
Monoclonal ANTI-FLAG M2 antibody produced in mouse	Sigma	Cat# F1804, Lot: SLBK1346V; RRID: AB_262044
Biological Samples		
adipocytes, SVF cells, serum samples from children undergoing elective surgery (Leipzig AT Childhood cohort)	Center for Pediatric Research Leipzig (CPL), University of Leipzig, Germany	N/A
DNA from children of the LIFE child study cohort	LIFE Research Center for Civilization Diseases, University of Leipzig, Germany	N/A
DNA from adults of the LIFE Adult study cohort	LIFE Research Center for Civilization Diseases, University of Leipzig, Germany	N/A
Chemicals, Peptides, and Recombinant Proteins		
PMA (Phorbol 12-myristate 13-acetate)	Sigma	Cat#P1585
murine TNFalpha	PeproTech	Cat#315-01A
murine IL-4	Sigma-Aldrich	Cat#SRP3211
human TRAIL	R&D Systems	Cat#375-TL
human TL1A	R&D Systems	Cat#1319-TL
human TNFalpha	R&D Systems	Cat#210-TA
Critical Commercial Assays		
Imprint Chromatin Immunoprecipitation kit	Sigma-Aldrich	Cat#CHP1-96RXN
Experimental Models: Cell Lines		
SGBS cells, human	Martin Wabitsch (University of Ulm, Germany)	N/A
3T3-L1, mouse	Peter Kovacs (University of Leipzig, Germany)	N/A
Chubs-S7, human	Assaf Rudich (Ben-Gurion University of the Negev, Israel)	N/A
Experimental Models: Organisms/Strains		
Zebrafish AB	European Zebrafish Resource Center (EZRC)	1175
Mouse C57BL/6NTac	Taconic	Black 6 (B6NTac)
Mouse db/db (BKS.Cg-m+/+Lep ^{db} /BomTac)	Taconic	Diabetic
MacGreen (CSF1R-eGFP ^{+/+}) mice on a C57BL/6 background	Sasmono et al., 2003	N/A
Oligonucleotides		
Oligonucleotides are summarized in Table S3 .	See Table S3	N/A
tmem18 morpholino (5'-CGAGAA TCTAATGTTACTCACAGAC (exon1-intron1))	This study; produced by Gene Tools	N/A

(Continued on next page)

Continued

REAGENT or RESOURCE	SOURCE	IDENTIFIER
non-targeting standard control morpholino (5'-CCTCTTACCTCAGTTACAATTATA)	Predesigned; Gene Tools	Cat#PCO-StandardControl-300
ON-TARGETplus SMARTpool small interfering (si)RNAs	Dharmacon	N/A
Recombinant DNA		
pGL3-PPARG1-p3000	Fajas et al., 1997	N/A
pGL3-PPARG2-p1000	Fajas et al., 1997	N/A
pCMV-TMEM18	OriGene	Cat#RC224267
Software and Algorithms		
GraphPad Prism 6	GraphPad Software	N/A
Statistica 10	Statsoft	N/A
SPSS, Version 24.0	IBM SPSS Statistics for Windows	N/A

RESOURCE AVAILABILITY

Lead Contact

Further information and requests for resources and reagents should be directed to and will be fulfilled by the Lead Contact, Antje Körner (antje.koerner@medizin.uni-leipzig.de).

Materials Availability

This study did not generate new unique reagents.

Data and Code Availability

This study did not generate or analyze datasets or code.

EXPERIMENTAL MODEL AND SUBJECT DETAILS

Leipzig AT Childhood cohort

Subcutaneous AT samples were obtained from 67 Caucasian children (0–18 years, 31 male, 36 female) undergoing orthopedic surgery (knee, leg, hip, arm, $n = 51$), herniotomy or orchidopexy (inguinal area, $n = 8$), abdominal surgery ($n = 4$), thoracic surgery ($n = 2$), back surgery ($n = 1$), or mammary reduction surgery ($n = 1$). Exclusion criteria were: diabetes, generalized inflammation, cardiovascular or peripheral artery disease, malignant disease, genetic syndromes. Written informed consent was obtained from all parents. The study was approved by the local ethics committee (Reg.No: 265-08, 265-08-ff, University of Leipzig) and is registered in the National Clinical Trials database (NCT02208141). BMI data were standardized to age- and sex-specific German reference data and are given as BMI standard deviation score (SDS). A cut-off of 1.28 and 1.88 SDS defined overweight and obesity in children ([Landgraf et al., 2012](#)). Levels of adiponectin, leptin, glucose and insulin were measured in the fasted state by a certified laboratory. HOMA-IR (homeostasis model assessment of insulin resistance) was calculated to evaluate insulin resistance ([Matthews et al., 1985](#)). Adipocytes and SVF cells were isolated by collagenase digestion as previously described ([Landgraf et al., 2015](#)). For analysis of cell size distribution, adipocytes were fixed in osmium tetroxide (Science Services, Munich, Germany) and adipocyte diameter was determined using a Coulter counter (Multisizer III; Beckmann Coulter, Krefeld, Germany). DNA from EDTA blood samples was isolated using the QIAamp DNA Blood MiniKit (QIAGEN Hilden, Germany). Genotyping of samples and imputation of SNP data were performed as part of the LIFE Child study ([Landgraf et al., 2016](#)).

LIFE Child study cohort

We included children of the LIFE Child Study cohort with available data from the German version of the Eating Disorder Examination-Questionnaire for Children (ChEDE-Q; $N = 1222$, 593 females, mean age 12.9y, SD = 2.2y, range = 7.1–18.8 years, mean BMI SDS = 0.29 ± 1.2) and from the Eating Disorder Examination interview for children assessing avoidant/restrictive food intake disorder ($N = 773$, 417 females, mean age 12.6y, SD = 2.7y, range = 7.5–18.8 years, mean BMI SDS = 0.34 ± 1.1). The ChEDE-Q questionnaire comprises 22 items building 4 subscales, i.e., restraint, eating concern, weight concern and shape concern ([Hilbert et al., 2013](#)). Participants are asked to rate on a 7-point frequency or intensity scale of different eating-related behaviors or thoughts considering the previous 28 days. The mean values of the four subscales were considered as outcome variables. In the ChEDE examination, the avoidant/restrictive food intake disorder (ARFID) was assessed with the ChARFID-Modul 1.0 interview. We considered ratings on food avoidance emotional disorder (FAED), selective eating and functional dysphagia as outcome variables.

The study was designed in accordance with the Declaration of Helsinki and under the supervision of the Ethics Committee of the University of Leipzig (Reg. No. 264-10-19042010) and is registered in the National Clinical Trials database (NCT02550236).

LIFE Adult study cohort

The adult sample was based on the LIFE-Adult-Study (Loeffler et al., 2015) and included 1144 randomly selected, community-dwelling volunteers with data from the Three Factor Eating Questionnaire or the Yale Food Addiction Scale (YFAS) available (542 females, mean age 63.4y, SD = 11y, range = 20–79 years, mean BMI = 27.5kg/m²). Participants consented to medical examination, anthropometric measurement, assessment of questionnaire data and genotyping. Exclusion criteria were stroke, cancer treatment in the last 12 months, neuroradiological findings of brain pathology, intake of centrally active medication and incomplete genomic or questionnaire data. The procedures were conducted according to the Declaration of Helsinki and approved by the University of Leipzig's ethics committee (registration-number: 263-2009-14122009).

The Three Factor Eating Questionnaire (Stunkard and Messick, 1985) provides information about self-rated eating behavior on three scales: disinhibition (tendency for dysregulated or emotional eating), cognitive restraint (cognitive control exerted over food intake) and hunger (occurrence of hunger feelings in daily life). Higher BMI has been consistently associated with higher levels of disinhibition and hunger (Bond et al., 2001; Cappelleri et al., 2009) while a more complex relationship of BMI and cognitive restraint has been proposed (Dietrich et al., 2014). The YFAS (Gearhardt et al., 2009) is a questionnaire designed to identify addictive tendencies toward certain type of foods and eating behavior (García-García et al., 2014). Here, we use the ordinal symptom score from the YFAS.

Animal models and maintenance

Animals were maintained under specific pathogen-free conditions and experiments were performed according to European guidelines and approved by the local ethics committee (Landesdirektion Sachsen, Leipzig, Germany). Zebrafish of the AB strain were maintained at 28°C at a 14h light: 10h dark cycle. Fluorescent bead assay and Nile red staining was performed in 9 day old zebrafish larvae. Expression analyses during early zebrafish development were performed between 1.5hpf and 9dpf. Expression analyses in zebrafish tissues were performed in adult male zebrafish at 6mpf. Mice of the C57BL/6NTac strain, the obese *db/db* strain as well as transgenic colony-stimulating factor 1 receptor (*Csf1r*) enhanced green fluorescent protein mice (CSF1R-eGFP+/-) on a C57BL/6 background were maintained at 22 ± 2°C on a 12h light/dark cycle. For qualitative RT-PCR analyses of *Tmem18* expression in different tissues of lean control (C57BL/6NTac) and obese *db/db* mice, one female and one male adult mouse per strain (10 to 12 weeks of age) were used. For IL-4 or TNFα treatment of AT explants 30 week-old, male mice, which had been on HFD starting from 6 weeks of age, were used.

Cell lines and culture conditions

Human Simpson–Golabi–Behmel syndrome (SGBS) cells were kindly supplied by Martin Wabitsch (University of Ulm, Germany) (Wabitsch et al., 2001). Cells were cultured in basal medium consisting of DMEM/Ham F12 medium (Life Technologies) supplemented with 10% fetal bovine serum, 33 μmol/l biotin and 17 μmol/l pantothenic acid. Human Chub-s7 cells were cultured in DMEM containing 4.5mM glucose, 10% FBS, 2mM L-glutamine, 100U/ml penicillin-streptomycin, until 24h post-confluence, with media change every other day. Murine 3T3-L1 cells were cultured in DMEM high glucose, 10% fetal bovine serum and antibiotics. Murine THP-1 monocytes were maintained in RPMI medium containing 100μM NEAA, 200μM L-Glutamin, 1mM Sodium pyruvate and 10% fetal calf serum. All cell lines were cultured at 37°C with 5% CO₂.

Cell lines were authenticated as adipose progenitor cell lines by their characteristic response to adipogenic inducers and the typical expression pattern of adipogenic marker genes.

METHOD DETAILS

Eating behavior and TMEM18 genotype

Genomic DNA was isolated from peripheral blood leucocytes using an automated protocol on the QIAGEN Autopure LS (QIAGEN, Hilden, Germany). Samples were genotyped using an Affymetrix Axiom Genome-Wide CEU 1 Array Plate comprising a total of 568 519 autosomal SNPs. We investigated rs7561317 (children: GG = 66.7% (n = 815), GT = 28.7% (n = 351), TT = 4.6% (n = 56); adults: GG = 67.2% (n = 769), GT = 29.1% (n = 333), TT = 3.7% (n = 42)). We grouped together homo- and heterozygotic non-risk allele carriers and used an independent samples t test to compare the BMI between these groups. In children, we used Mann-Whitney U-test to compare groups considering all eating behavior-related outcomes because of the skewed distributions of the scales. To test if results were different between females and males, we run additional tests in these groups separately. As age was similarly distributed between the genotype groups in both subsamples (independent t tests, all *t* < 1.5, all *p* > 0.13), confounding by age can be regarded negligible. In adults, we performed a multivariate analysis of variance (MANOVA) with group as predictor, disinhibition (log-transformed), hunger (log-transformed) and cognitive restraint measures from the TFEQ as dependent variables and age and sex as confounders. For the YFAS symptom score we used the Mann-Whitney U-test to compare groups because of the ordinal nature of the scale.

RNA isolation and RT-PCR analysis

Total RNA from SGBS and 3T3-L1 cells, zebrafish or mouse tissues was isolated using the RNeasy Mini Kit (QIAGEN,) including on-column DNA digestion according to the manufacturer's instructions. An aliquot of 500ng of RNA was reverse transcribed into cDNA using M-MLV Reverse Transcriptase (Invitrogen, Darmstadt, Germany) and random hexamer primers (Promega, Madison, WI, USA).

Total RNA isolation, cDNA synthesis and quantitative *real-time* PCR from 396 subcutaneous and 408 visceral AT samples ($n = 275$ paired samples from the same individuals) from 529 adults included in the previously described GOBB - German Obesity BioBank (Bernhard et al., 2013; Langhardt et al., 2018) as well as adipocytes and SVF cells from 67 subcutaneous AT samples from children of the Leipzig AT Childhood cohort were performed as previously described (Landgraf et al., 2016; Rockstroh et al., 2015).

Total RNA from chub-s7 cells was performed by Assaf Rudich's lab using the RNeasy lipid tissue minikit (QIAGEN). 2 μ g of RNA were reverse-transcribed with a high capacity cDNA reverse transcriptase kit (Life Technologies).

For zebrafish and SGBS cells, the copy number of each sample was determined from a standard curve and normalized to the mean of the two reference genes *beta-actin* (*actb*, *ACTB*) and *TATA-box-binding protein* (*tbp*, *TBP*). For adipocytes and SVF cells from children, *TMEM18* copy number of each sample was determined from a standard curve and normalized to the mean of the three reference genes *ACTB*, *TBP* and hypoxanthine phosphoribosyltransferase 1 (*HPRT*). Gene expression levels in subcutaneous and visceral AT samples from adults were normalized to expression of the reference gene *TBP*. For chubs-s7 adipocytes, gene expression levels were measured using *real-time* PCR amplification with Taqman technology (Upl, Roche). Relative gene expression was obtained after normalization to the endogenous control genes *phosphoglycerate kinase 1* (*PGK1*) and *peptidylprolyl isomerase A* (*PPIA*) (Neville et al., 2011), using the formula $2^{-\Delta\Delta C_t}$. Primer and probe sequences used for quantitative *real-time* PCR are listed in Table S3.

For qualitative RT-PCR analyses of *Tmem18* expression in different tissues of lean control (C57BL/6NTac) and obese *db/db* mice, cDNA samples of one female and one male mouse per strain were pooled. *Tmem18* expression was analyzed using primers directed against full-length *Tmem18* cDNA, detection of *glyceraldehyde-3-phosphate dehydrogenase* (*Gapdh*) expression served as loading control. Primers used for RT-PCR analyses were: 5'-ACTGGGATCCATGTCGTCGCCATACACTCAGT and 5'-ACTGCTCGAGTT ACTCTTCCTTCCTCCTCC for *Tmem18*, 5'-AGGCCGGTGCTGAGTATGTC and 5'-TGCCTGCTTACCACCTTCT for *Gapdh*.

In situ hybridization analysis

Zebrafish embryos were obtained from matings of wild-type fish of the AB strain. Embryos were raised at 28°C and staged according to Kimmel et al. (1995). Whole-mount *in situ* hybridizations were performed using digoxigenin-labeled riboprobes in antisense and sense orientation as previously described (Hauptmann and Gerster, 1994). The full length coding region of *tmem18* was amplified with the following primers: 5'-ACTGGGATCCATGACAGCATCAACACTAAAAA and 5'-ACTGCTCGAGCTATTGTGTTTCT TGTGGTTC. The cDNA fragment was cloned into pCRII-TOPO (Invitrogen). The cDNA template for the *pparg* *in situ* probe was kindly provided by Yann Gibert (Deakin University, Melbourne, Australia). *In vitro* transcription was performed using the DIG RNA Labeling Kit (SP6/T7; Roche, Mannheim, Germany).

Morpholino injection of zebrafish embryos

Injections into zebrafish embryos were performed as described (Landgraf et al., 2010). Briefly, morpholino antisense oligonucleotides (Gene Tools, Philomath, OR, USA) were diluted to a concentration of 0.5mM in water with 0.1% phenol red (Sigma), and 2nl (8ng per embryo) were injected into the yolk of 1- to 2-cell embryos. Morpholinos (MO's) were directed against splice donor or acceptor sites of the pre-mRNA. The *tmem18* MO sequence is as follows: 5'-CGAGAATCTAATGTTACTCACAGAC (exon1-intron1). A non-targeting standard control MO (5'-CCTCTTACCTCAGTTACAATTATA; Gene Tools) was used as a control for unspecific effects.

For mRNA rescue experiments, *tmem18* mRNA was synthesized using the mMESSAGE mMACHINE kit (Life Technologies, Darmstadt, Germany). Zebrafish embryos injected with 8ng *tmem18* MO were subsequently injected with 150pg of *tmem18* mRNA.

Injected zebrafish embryos were kept in Danieau's embryo medium in an incubator at 30°C. At 5dpf zebrafish larvae were placed in a recirculation system and fed twice daily with dry food (Sera micron) and egg yolk powder (Sigma).

Nile red staining of zebrafish larvae

In order to visualize visceral adipocytes as individual cells and to quantify their number zebrafish larvae were stained with the lipophilic dye Nile red and imaged using fluorescence microscopy according to Flynn et al. (2009) with slight modifications. Briefly, zebrafish larvae at 9dpf were fixed overnight in 4% paraformaldehyde. After washing in PBS, larvae were incubated in Nile red solution (0.5 μ g/ml in PBS) for 2h at 30°C in the dark, washed in PBS, mounted in 1% methylcellulose and imaged using an AxioZoom.V16 microscope (Zeiss, Jena, Germany). Adipocytes in the visceral region were counted and eye diameter of each zebrafish larva was measured using ImageJ software (National Institutes of Health, Maryland, USA).

Eating behavior of zebrafish larvae

For analysis of eating behavior, a fluorescent bead assay was employed (Farber et al., 2001). Larvae at 9dpf were placed in tank water containing fluorescent latex microspheres (0.0025% Fluoresbrite plain YG 2.0 μ m; Polysciences Inc., Eppelheim, Germany) for 1h, washed, and imaged using an Axio Zoom.V16 microscope (Zeiss, Jena, Germany).

In vitro adipocyte differentiation

SGBS cell differentiation was induced under serum-free conditions by treating confluent cells with medium comprising 20nM insulin, 100nM hydrocortisone, 0.2nM tri-iodothyronine and 0.13nM apo-transferrin. For the first 4 days of differentiation, the medium was additionally supplemented with 25nM dexamethasone, 500μM isobutyl-1-methylxanthine and 2μM rosiglitazone.

3T3-L1 cells were differentiated as previously described (Zebisch et al., 2012). Briefly, cells were grown in DMEM high glucose, 10% fetal bovine serum and antibiotics. For differentiation, confluent cells were induced for 2 days by adding 1μg/ml insulin, 500μM isobutyl-1-methylxanthine, 0.25μM dexamethasone and 2μM rosiglitazone before being maintained for another two days in culture medium supplemented with 1μg/ml insulin and for an additional 6 days in culture medium.

Protein extraction and immunoblotting

Preparation of nuclear and cytoplasmic extracts from different time points of SGBS adipocyte differentiation was performed as previously described (Musharraf et al., 2014). For whole cell extracts, cells were lysed in RIPA lysis buffer (50mM Tris pH7.5, 150mM NaCl, 1% Triton X-100, 0.1% SDS). Equivalent amount of protein was resolved by SDS-polyacrylamide gel electrophoresis and detected by immunoblotting using anti-TMEM18 (ab100954; abcam, Cambridge, UK), anti-PPARγ (C26H12; Cell Signaling, Frankfurt, Germany), or anti-FLAG M2 (F1804; Sigma, Taufkirchen, Germany) antibodies. Equal loading was confirmed by detection of β-Actin (A5316; Sigma), c-JUN (60A8; Cell Signaling), or G6PD (Cell Signaling).

Immunocytochemistry

SGBS cells were grown on coverslips until reaching confluency and differentiated as described above. Before adipogenic induction (d0) and after adipocyte differentiation (d8), cells were fixed in 4% PFA. Permeabilisation of cells was performed using 0.25% Triton X-100 or 40μg/ml Digitonin and TMEM18 was detected using anti-TMEM18 (ab100954; abcam) in combination with a Dylight488-conjugated donkey anti-rabbit antibody (Jackson ImmunoResearch, Cambridgeshire, UK). A rabbit anti-GFP antibody (2555, Cell Signaling) was used as a control antibody to exclude unspecific signals. After mounting with IS Mounting Medium DAPI (Dianova, Hamburg, Germany), cells were visualized using a fluorescence microscope (Zeiss).

siRNA-mediated knockdown

SiRNA transfections were performed using the Neon Transfection System 100 μL Kit (Invitrogen). Electroporation was optimized to pulse voltage 1300V, pulse width 20ms, pulse number 2 and a cell density of 6×10^6 cells/ml (Bernhard et al., 2013). Gene-specific ON-TARGETplus SMARTpool small interfering (si)RNAs and ON-TARGETplus control reagents (Dharmacon, Lafayette, LA, USA) were used at a final concentration of 500nM. After electroporation, 100,000 cells/well for SGBS or 150,000 cells/well for 3T3-L1 cells were seeded in 12-well format and differentiated into mature adipocytes as described above. Efficient knockdown was confirmed using quantitative *real-time* PCR. For Oil Red-O staining, adipocytes at day 8 post-induction were fixed in Roti-Histofix 4% (Carl Roth GmbH, Karlsruhe, Germany), washed with PBS and stained with Oil Red-O solution (0.3% in 60% isopropanol) for 15 min.

Luciferase reporter assay

Luciferase reporter assays were based on a previous study by Fajas et al. (1997). Luciferase reporter constructs containing human *PPARG1* (pGL3-PPARG1-p3000) or *PPARG2* (pGL3-PPARG2-p1000) promoter fragments were kindly provided by Johan Auwerx (Ecole Polytechnique Fédérale, Lausanne, Switzerland). Deletion constructs of the *PPARG1* promoter were generated by digestion of the full-length luciferase reporter construct with indicated restriction enzymes followed by blunting and re-ligation. Successful deletion was confirmed by sequencing.

Transfection of 3T3-L1 cells for luciferase reporter assays was performed using Fugene HD transfection reagent (Promega). 3T3-L1 cells (1×10^5) were seeded into 6-well dishes and transfected on the following day with 1 μg pGL3-basic or pGL3-*PPARG* reporter construct and 1 μg pCMV-*TMEM18* expression plasmid (Myc-DDK-tagged; OriGene, Rockville, MD, USA) or empty vector. To normalize for transfection efficiency, 0.5 μg pRL-CMV control plasmid was added to each sample. At 48h post-transfection, cells were harvested, and luciferase activities were determined using the dual-luciferase reporter assay (Promega).

Chromatin immunoprecipitation (ChIP)

1×10^6 SGBS preadipocytes were electroporated with 5μg of pCMV-*TMEM18* expression vector and cultured in growth medium for 48h. Harvesting of cells, cross-linking of DNA-protein complexes, shearing of chromatin (target fragment size 500bp), immunoprecipitation, cross-linking reversal and DNA isolation were performed using the Imprint Chromatin Immunoprecipitation kit (Sigma). 2×10^5 cells were used per sample. TMEM18 protein was precipitated using mouse anti-FLAG M2 antibody (F1804; Sigma). Mouse control IgG and anti-RNA POL II antibody (provided in the kit) were used as negative and positive control, respectively. The purified DNA was amplified using primers specific for the *GAPDH* promoter (Imprint, Sigma) or the following primers specific for different regions of the *PPARG1* promoter: F1 forward 5'-GGAACCCTGACACATTGCTG and reverse 5'-GTTGTTTCTACTTTTATGGGCTA, F2 forward 5'-GTCCAGAATAGGTAAATCTATAG and reverse 5'-GTGCCATCATCACCAAATCTA, F3 forward 5'-GACACAGCAACACCCTGTC and reverse 5'-AGGCAGCGATGCCTGAGG.

Treatment of cells with macrophage conditioned media

Murine THP-1 monocytes were treated with 100ng/μl PMA (Sigma) under serum-free conditions in RPMI basal medium containing 0.5% bovine serum albumin or left untreated (control) for 24h. Subsequently, cells were washed with PBS three times and fresh basal medium containing 0.5% bovine serum albumin was added. Macrophage-conditioned medium was collected after 48h of incubation and added to SGBS cells, which had been undergoing adipocyte differentiation for 10 days. Incubation of SGBS cells with macrophage-conditioned medium was performed for 24h before harvesting cells for RNA isolation and RT-PCR analyses.

IL-4 and TNFalpha treatment of AT explants

Organotypic AT culture and IL-4 or TNFalpha treatment was performed as previously described (Braune et al., 2017). Briefly, heterozygote transgenic colony-stimulating factor 1 receptor (*Csf1r*) enhanced green fluorescent protein mice (CSF1R-eGFP+/-) on a C57BL/6 background were fed a high-fat diet (60% kcal fat; Ssniff-Spezialdiäten GmbH; Soest, Germany) starting at 6 weeks of age. After 24 weeks of HFD, male mice were killed and the rostral part of the epididymal fat pad was exposed and further processed sterilely. The fat pad was dissected into 1mm x 1mm explants using a sterile razor blade. Explants were cultured for 48h in RPMI medium (Sigma-Aldrich, Deisenhofen, Germany) supplemented with 1% insulin-transferrin-selenium mixture and antibiotics (100U/ml penicillin and streptomycin; all reagents from Sigma-Aldrich) and further stimulated by either 50ng/ml of murine TNFalpha or IL-4 (PeproTech, Hamburg, Germany and Sigma-Aldrich). All experiments were approved by the local authorities.

TRAIL and TL1A treatment of chub-s7 adipocytes

Chub-s7 cells were cultured until 24h post-confluence and differentiation was induced by adding 1mM dexamethasone, 0.5mM IBMX, 10mg/ml of insulin and 10mM of rosiglitazone to the medium for 14-21 days, until the appearance of adipocyte morphology. For quantitative real-time PCR experiments, differentiated chub-s7 adipocytes were treated for 24h in serum-free media, with the addition of 0, 5 or 25ng/ml TRAIL or TL1A (hrTRAIL and hrTL1A by R&D, respectively).

TNFalpha treatment of differentiated SGBS cells

SGBS preadipocytes were cultured and induced to adipocyte differentiation using the protocol as previously described. At day 8 post adipogenic induction SGBS cells were stimulated with 10ng/ml of recombinant human TNFalpha (R&D Systems; Minneapolis (MN); USA) in differentiation medium for 6h and 24h before harvesting cells for RNA isolation and RT-PCR analyses.

For *TMEM18* overexpression rescue experiments SGBS preadipocytes were transfected using Eugene HD transfection reagent (Promega). Briefly, SGBS cells (7.5×10^4) were seeded into 12-well dishes and transfected on the following day with 1 μg pCMV-*TMEM18* expression plasmid or empty vector. 48h post-transfection, adipocyte differentiation was induced. Cells were treated with TNFalpha at day 8 of differentiation as described above and mRNA expression was compared to untreated cells.

QUANTIFICATION AND STATISTICAL ANALYSIS

Statistical analyses of cell culture and zebrafish experiments were performed using GraphPad Prism 6 (GraphPad Software, San Diego, CA, USA). Statistical analyses of human AT samples were performed using Statistica 10 (StatSoft, Tulsa, OK). Statistical analyses on human eating behavior were performed in SPSS (IBM Corp. Released 2012. IBM SPSS Statistics for Windows, Version 24.0).

Data that did not adhere to Gaussian distribution were log-transformed before analyses. Parametric tests (Pearson correlation analysis, Student's t test, one-way ANOVA) were applied for quantitative traits and χ^2 test for categorical variables. In the group stratification for obesity, patients with overweight and patients with obesity were combined. For statistical analyses of *TMEM18* expression according to obesity risk genotype minor allele carriers were combined into one group and compared to homozygous major allele carriers using Student's t test. Statistical tests are indicated in the results section or the figure legends.

To confirm results each *in vitro* (cell culture, mouse tissue treatment) and *in vivo* experiment (zebrafish expression and injection) was independently repeated at least 3 times. In addition, wherever suitable, i.e., quantitative gene expression analyses of cell culture and zebrafish experiments, luciferase reporter assays, measurement was performed in technical replicates.

Supplemental Information

The Obesity-Susceptibility Gene *TMEM18* Promotes

Adipogenesis through Activation of *PPARG*

Kathrin Landgraf, Nora Klöting, Martin Gericke, Nitzan Maixner, Esther Guiu-Jurado, Markus Scholz, A. Veronica Witte, Frauke Beyer, Julian T. Schwartz, Martin Lacher, Arno Villringer, Peter Kovacs, Assaf Rudich, Matthias Blüher, Wieland Kiess, and Antje Körner

A

Human : -----MPSAFSVSSFP-----VSIPAVLTQTDWTEPWLMGLATFHALCVLLTCLSSRSY : 49
 Mouse : -----MSAYSVRSEF-----VSIPAVIMETDWTEPWLLGLLAFHLLCLLLTCLSSORY : 49
 Zebrafish : MTASNTKNASAIPTDKESNVRITSIWTFLLQSDWSEPWLMALLAFHVFCFAFTLLSCYY : 60

Human : RLQIGHFLCLVILVYCAEYINEAAMNWRLFASKYQYFDSRGMFISIVFSAPLLVNAMIIV : 109
 Mouse : KLQIGHFLCLVILVYSAEYINEAAVNWRLFASKYQYFDSRGMFISLVFSAPLLFNAMLIV : 109
 Zebrafish : RIQICHFLMVAMVYSAEYLNEAAMNWRFSKFOYFDSKGMFISLVYSVPLLNTVIIV : 120

Human : VMWVWKTLLNMTDLKNAQERRKEKKRRRKED- : 140
 Mouse : IMWVRKTLTVMTDLKTLQERRKERRRRRKEE- : 140
 Zebrafish : AVWVWRTEFSLMTLKLILQLKRKAARENHKKTQ : 152

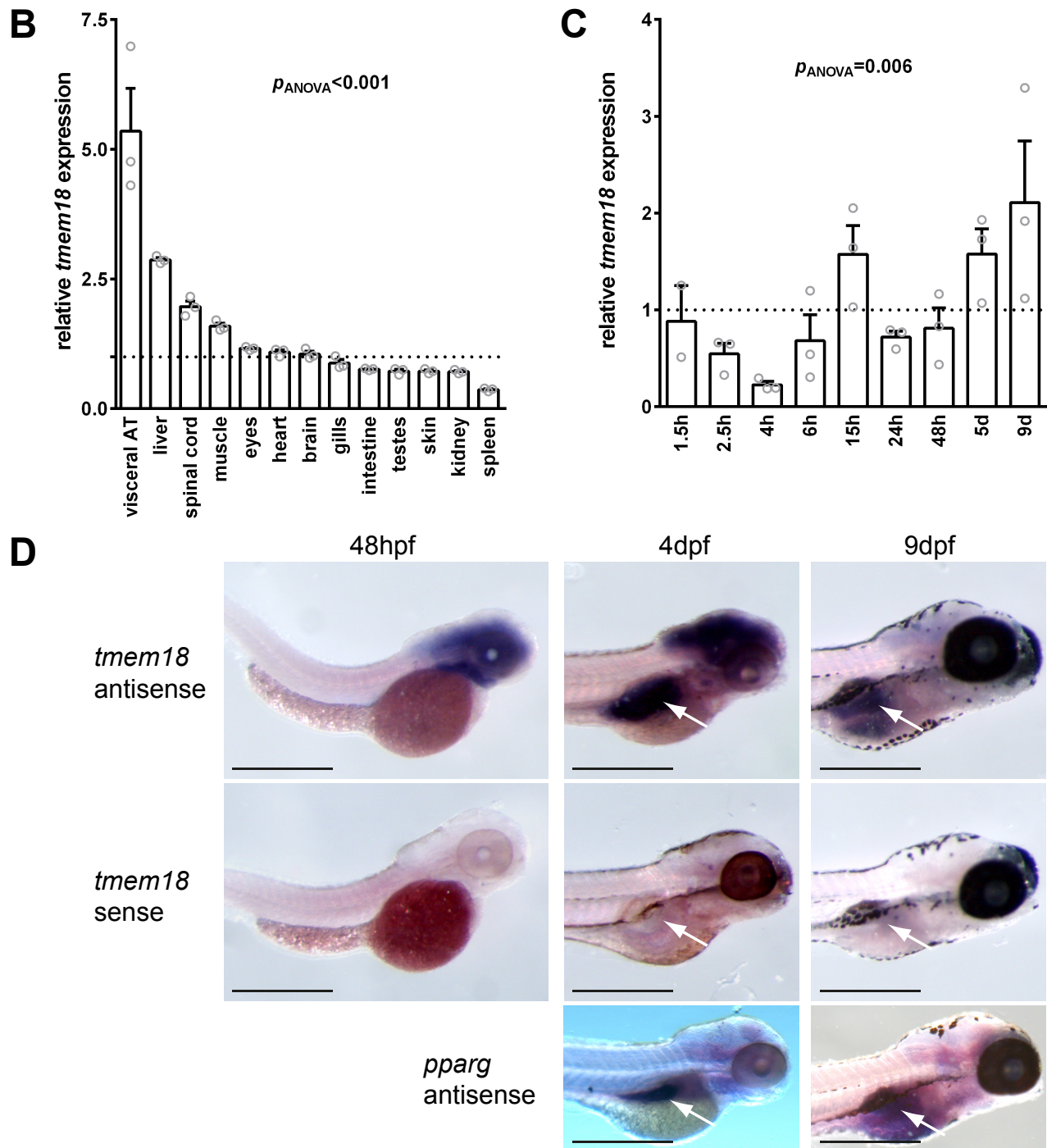


Fig. S1. *TMEM18* is conserved in zebrafish and co-expressed with *pparg*. Related to Figure 2. (A) Tmem18 protein sequences were aligned using the ClustalW algorithm. Zebrafish Tmem18 protein is highly similar compared to human (64%) and mouse (69%). (B) The expression profile of *tmem18* in different tissues of adult male zebrafish at 6mpf ($n=3$, pooled) was analyzed by quantitative *real-time* PCR and showed highest expression in visceral AT. Expression levels were quantified in triplicates and were standardized to the median expression across all tissues (dotted line). Data are presented as mean \pm SEM. (C) During early zebrafish development overall *tmem18* mRNA levels were downregulated between 1.5hpf and 4hpf followed by a steady increase till 9dpf. Data were determined from 3 independent experiments (20 pooled embryos per time point) each measured in triplicates and are presented as mean \pm SEM. (D) Localization of *tmem18* mRNA expression during early zebrafish development (48hpf, 4dpf, 9dpf) was analyzed by whole-mount *in situ* hybridization using gene-specific probes in antisense or sense orientation (scale bar 500 μ m). *Tmem18* was expressed in the brain and the region surrounding the swim bladder (white arrows), where *pparg* expression was also detected. mpf, months post fertilization; hpf, hours post fertilization; dpf, days post fertilization.

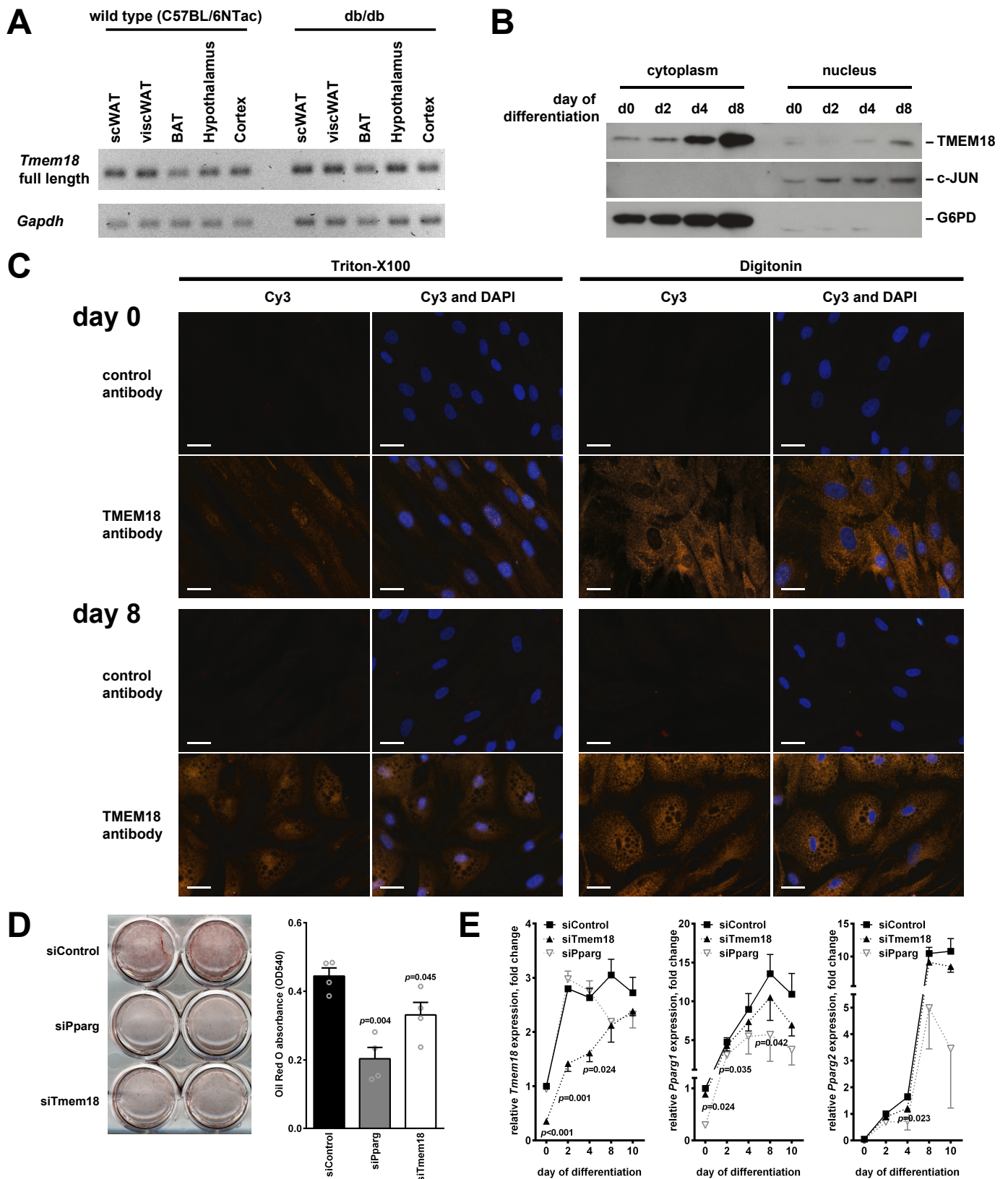


Fig. S2. *Tmem18* is localized in both cytoplasm and nucleus of adipose progenitor cells and involved in adipocyte differentiation. Related to Figure 3. (A) Expression of *Tmem18* was detected in adipose and brain tissues of wild type (C57BL/6NTac) and db/db mice using RT-PCR. Analysis of TMEM18 protein localization before adipogenic induction (=d0) and during adipocyte differentiation (d2, d4, d8 of differentiation) by cellular fractionation and immunoblot (B) or immunofluorescence (C) showed that TMEM18 protein is detectable in both cytoplasm and nucleus of human SGBS cells. Nuclear localization of TMEM18 was confirmed by comparing SGBS cells permeabilized with Triton-X100 (permeabilizes nucleus) and Digitonin (does not permeabilize nucleus) and TMEM18-specific immunofluorescence (scale bar 50µm). (D) Adipocyte differentiation of murine 3T3-L1 cells was reduced after siRNA-mediated knockdown of *Pparg* and *Tmem18* as indicated by Oil Red-O staining at day 8. (E) *Tmem18* knockdown reduced *Pparg1* expression during early and late adipocyte differentiation of 3T3-L1 cells and *Pparg2* expression during late adipocyte differentiation. Data are given as mean±SEM. Significant p-values are indicated for siTmem18 compared to siControl ($p<0.05$). WAT, white adipose tissue; sc, subcutaneous; visc, visceral; BAT, brown adipose tissue.

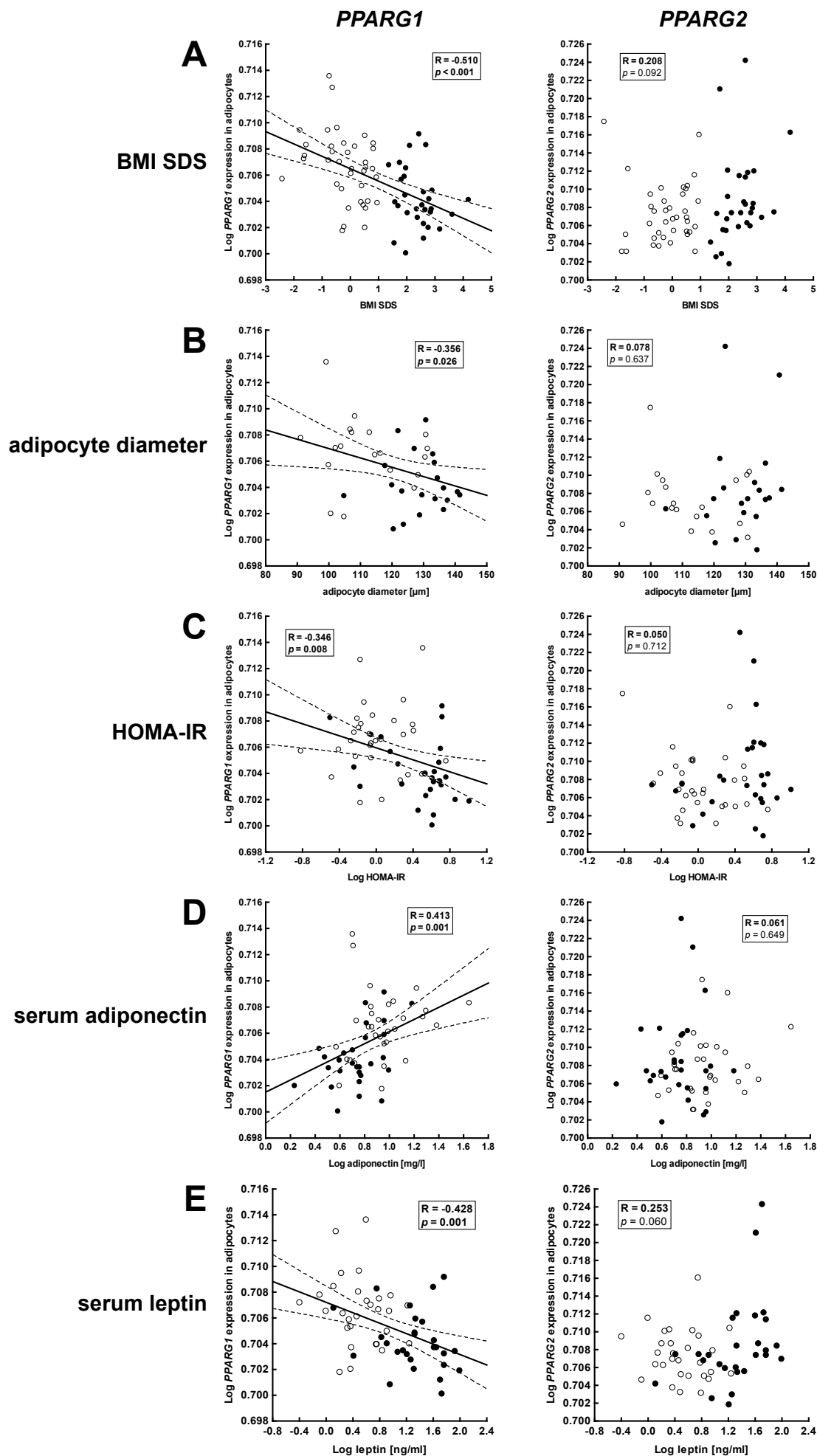


Fig. S3. *PPARG1* expression in adipocytes is associated with obesity and related parameters in children *in vivo*. Related to Figure 3. Adipocyte *PPARG1* but not *PPARG2* expression was significantly correlated to BMI SDS (A), adipocyte diameter (B), HOMA-IR (C), and adiponectin (D) and leptin (E) serum levels in children. Pearson correlation coefficient R and p-value are given in each scatter plot. Significant p-values (p<0.05) are indicated in bold. Lean children are represented as open, children with obesity as closed circles.

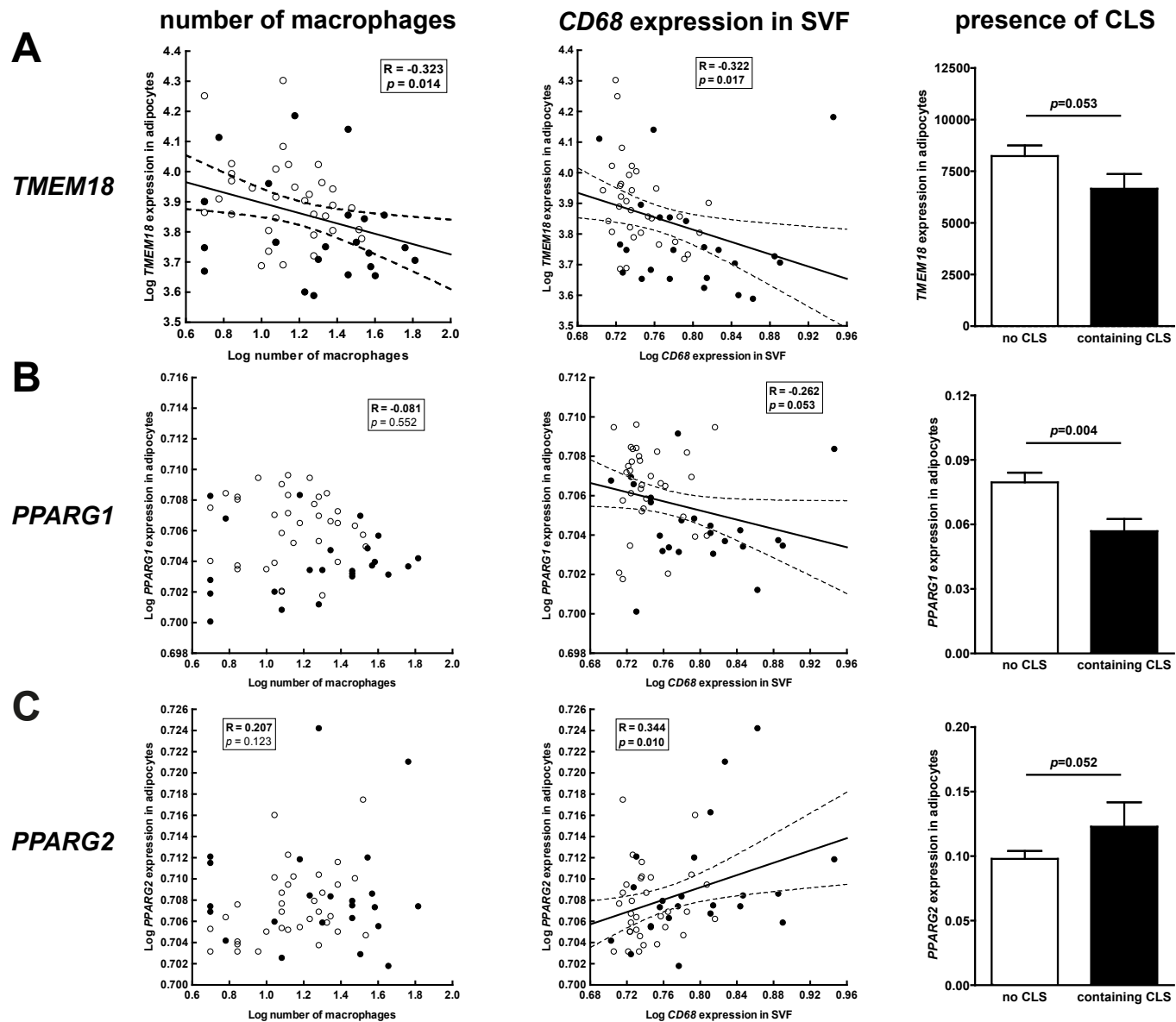


Fig. S4. Both adipocyte *TMEM18* and *PPARG1* expression are negatively associated with AT inflammation *in vivo*. Related to Figure 4. Associations of *TMEM18* (A), *PPARG1* (B) and *PPARG2* (C) expression in adipocytes with parameters of AT inflammation are shown. Only adipocyte *TMEM18* expression was associated with the number of CD68-positive macrophages in subcutaneous AT samples of children, while there was no association of adipocyte *PPARG1* or *PPARG2* expression with macrophage infiltration. In line with this, adipocyte *TMEM18* expression negatively correlated with *CD68* expression in SVF cells. Similarly, *PPARG1* negatively correlated with SVF *CD68* expression by trend, while *PPARG2* showed a positive association. Pearson correlation coefficient *R* and *p*-value are given in each scatter plot. Lean children are represented as open, children with obesity as closed circles. In addition, both *TMEM18* and *PPARG1* expression in adipocytes were lower in AT samples containing CLS compared to samples without CLS, while *PPARG2* expression appeared to be increased in AT samples containing CLS. Data are given as mean±SEM and *p*-values are indicated.

Table S1. Related to Fig. 1. Characteristics of the Childhood Adipose Tissue Cohort (n=67)

	Lean			Obese			<i>p</i>
	<i>n</i>	Mean±SEM	Range	<i>n</i>	Mean±SEM	Range	
Male/Female (% male)		20/18 (52.6)			11/18 (37.9)		0.232
Age [years]	38	9.5±0.9	1.1–18.3	29	12.9±0.7	4.8–18.0	0.004
PH	33	2.3±0.3	1–6	27	3.4±0.3	1–6	0.016
BMI SDS	38	-0.2±0.1	-2.4–0.9	29	2.4±0.1	1.4–4.2	<0.001
Adipocyte diameter [µm]	19	112.3±2.9	90.9–131.2	20	130.0±2.0	104–141.5	<0.001^a
Macrophages per 100 adipocytes	34	10.4±1.3	0–29	23	20.2±3.6	0–60	0.005
<i>CD68</i> expression	32	0.6±0.1	0.1–1.6	23	1.3±0.2	0–3.8	<0.001^a
Number of children with CLS (%)	34	3 (8.8%)		23	12 (52.2%)		<0.001
Adiponectin [mg/l]	31	10.4±1.4	3.7–43.8	28	6.1±0.5	1.7–15.1	0.007^a
Leptin [ng/ml]	29	4.6±0.8	0.4–17.5	27	31.8±4.9	1.3–99.0	<0.001^a
HOMA-IR	32	1.4±0.2	0.04–5.6	27	4.0±0.4	0.3–10.1	<0.001^a

Data are given as mean ± SEM. For gender and occurrence of CLS, statistical significance was analysed by Chi-square test. Statistical significance for differences between groups was determined by Students *t* test. Significant *p* values are indicated in bold. PH, pubertal stage; BMI, body-mass index; SDS, standard deviation score; CLS, crown-like structures; HOMA-IR, homeostasis model assessment of insulin resistance. ^aStatistical analyses were performed for log-transformed parameters.

Table S2. Related to Fig. 1. Association of obesity-associated risk alleles with *TMEM18* mRNA levels in adipocytes and stroma vascular cells of lean and obese children (n=67).

variant	relative mRNA levels stratified by genotype				P
		0	1	2	
rs7561317 downstream	genotype	AA	AG	GG	
	lean	6177±230 n=2	7061±538 n=9	9078±658 n=27	0.030
	adipocytes				
	obese	6940 n=1	6578±1133 n=8	6645±651 n=20	0.966
	lean	9724±610 n=2	12264±922 n=9	14107±815 n=27	0.106
	SVF				
	obese	9541 n=1	13415±848 n=8	12866±840 n=20	0.769
rs17729501 3'-UTR	genotype	CC	CT	TT	
	lean	12076 n=1	10710±1653 n=6	7893±495 n=31	0.014
	adipocytes				
	obese	n=0	8392±2309 n=4	6645±651 n=25	0.212
	lean	15591 n=1	12114±1399 n=6	13627±737 n=31	0.563
	SVF				
	obese	n=0	11945±593 n=4	12866±840 n=25	0.714
rs10168696 intron3	genotype	CC	CT	TT	
	lean	5408 n=1	7881±532 n=8	8709±641 n=29	0.436
	adipocytes				
	obese	5917±620 n=3	6673±1262 n=8	6737±688 n=19	0.832
	lean	9268 n=1	12565±1250 n=8	13825±757 n=29	0.273
	SVF				
	obese	15093±771 n=3	14280±1715 n=8	12049±670 n=19	0.094

Data are presented as mean±SEM. 0, homozygote for minor allele; 1, heterozygote; 2, homozygote for major allele. For statistical analyses minor allele carriers were combined into one group and compared to major allele carriers using Student's *t* test. Significant *p* values are indicated in bold.

Table S3. Related to Methods. Primer and probe sequences for quantitative *real-time* PCR

Target Gene	Forward Primer	Reverse Primer	Probe
Zebrafish			
<i>tmem18</i>	Predesigned Assay		Dr03147200_m1
<i>fabp10a</i> (Lin et al., 2014)	CACCTCCAAACTCCTGGAA	TTCTGCAGACCAGCTTTCCT	SYBR Green
<i>ifabp</i>	Predesigned Assay		DR03086825_g1
<i>cebpb</i> (Hall et al., 2012)	TCCGTCTGCCGCAAT	TAAAAACCGGCCACTTCCAT	SYBR Green
<i>cebpd</i>	Predesigned Assay		Dr03106022_s1
<i>cebpa</i>	Predesigned Assay		Dr03105987_s1
<i>pparg</i>	GCTGCACAGGCGCTTCA	CTCCAGCTCCTCCAGTTCCA	CAGAAAAGCTTCACTC TCCGCTGATATGGTG
<i>lpl-b</i>	CTGAGGGCTCTCGTTCATAAA GA	AATCCATCAAAGACTGTAAC TCAATACA	CTCTCAAACATACCC GTGACCGTCCATC
<i>fabp11a</i>	GGTTGACAAATTCGTAGGAAC GT	AACCCACACCTATAGCCTTCAT G	AATGACCACCAGCGA CAACTTTGACGA
<i>adipoq B</i>	GGATGGGCGGTGTTCCA	ACCTGCTTACCTTGATCTCCT T	CACACCTGGGCACAG TGGAAAACCTG
<i>lipe</i>	CGGCAAGGACAGGACAGT	GCATGGAGAAAAGAGGAGCT	SYBR Green
<i>actb</i>	TCCCCTTGTTACAATAACCTA CTAA	CATACCGGAGCCGTTGTCA	AGCGATTTCTCATCC ATGGCTGTGT
<i>tbp</i>	CCTGCGAATTATCGTTTACGTC TT	ACGGCATCATAGGACTGAAAA TG	TTGCTTCATAACCTGT CAGCATGGAGCA
Mouse			
<i>Tmem18</i>	GCTCTGTGAATGGCTTATCTG	CTCTGTCACCTCAAATCTCTAA AG	SYBR Green
<i>Pparg1</i>	TGAAAGAAGCGGTGAACCAC TG	TGGCATCTCTGTGTCAACCAT G	TAAAAACAAGACTA CCCTTTACTGAA
<i>Pparg2</i>	TGGCATCTCTGTGTCAACCAT G	GCATGGTGCCTTCGCTGA	SYBR Green
<i>Actb</i>	GCTCTGGCTCCTAGCACCAT	GCCACCGATCCACACCGCGT	TCAAGATCATTGCTC CTCCTGAGCGC
<i>Tbp</i>	AATCTTGGCTGTAACTTGAC CTAAAG	CGTGGCTCTCTATTCTCATGA TG	TCGTGCAAGAAATGC TGAATATAATCCCAA GC
Human: Analyses of SGBS cells and patient AT samples			
<i>TMEM18</i>	GTCATCTTAGTCTACTGTGCTG AATACATC	CCCCCTGGAGTCGAAATACTG	CTCCAGTTCATCGCA GCCGCCT
<i>PPARG1</i> (Bruedigam et al., 2008)	GTGGCCGCAGATTTGAAAGA AG	TGTCAACCATGGTCATTTG	SYBR Green
<i>PPARG2</i> (Bruedigam et al., 2008)	CAAACCCCTATTCCATGCTGTT	AATGGCATCTCTGTGTCAACC	SYBR Green
<i>CEBPB</i>	Predesigned Assay		Hs00270923_s1
<i>CEBPD</i>	Predesigned Assay		Hs00270931_s1
<i>CEBPA</i>	Predesigned Assay		Hs00269972_s1
<i>SREBF1</i>	Predesigned Assay		Hs01088679_g1
<i>LPL</i>	Predesigned Assay		Hs00173425_m1
<i>FABP4</i>	Predesigned Assay		Hs01086177_m1
<i>PLIN1</i>	Predesigned Assay		Hs00160173_m1
<i>ADIPOQ</i>	GGCCGTGATGGCAGAGAT	CCTTCAGCCCCGGGTACT	CGATGTCTCCCTTAG GACCAATAAGACCTG G
<i>LIPE</i>	Predesigned Assay		Hs00943410_m1

<i>SLC2A4</i>	Predesigned Assay		Hs00943410_m1
<i>LEP</i>	Predesigned Assay		Hs00943410_m1
<i>ACTB</i>	TGAGCGCGGCTACAGCTT	CCTTAATGTCACGCACGATTT	ACCACCACGGCCGAGCGG
<i>TBP</i>	TTGTAACTTGACCTAAGACCATTGC	TTCGTGGCTCTCTTATCCTCATG	AACGCCGAATATAATCCCAAGCGGTTTG
<i>HPRT</i>	GGCAGTATAATCCAAAGATGGTCAA	GTCTGGCTTATATCCAACACTTCGT	CAAGCTTGCTGGTGA AAAGGACCCC
Human: Analyses of chubs-s7 cells			
<i>TMEM18</i>	TCCGCCTTCTCTGTCAGC	GGCTCAGTCCAGTCCGTCT	UPL probe 89, Roche (04689143001)
<i>PPARG1</i>	GACAGGAAAGACAACAGACA AATC	GGGGTGATGTGTTTGAAC TTG	UPL probe 7, Roche (04685059001)
<i>PPARG2</i>	TCCATGCTGTTATGGGTGAA	TGTGTCAACCATGGTCAT TTC	UPL probe 14, Roche (04685130001)
<i>PPIA</i>	ATGCTGGACCCAACACAAAT	TCTTTCAC TTTGCCAAACACC	UPL probe 48, Roche (04688082001)
<i>PGK1</i>	CTGTGGCTTCTGGCATACT	CGAGTGACAGCCTCAGCATA	UPL probe 42, Roche (04688015001)

Primers and probes are given in 5'-3' direction. Predesigned assays were obtained from Life Technologies.